MINIMIZATION OF FOUR-WAVE MIXING IN WAVELENGTH DIVISION MULTIPLEXING OPTICAL COMMUNICATION SYSTEMS

ISMAILA ABIOLA ARANSIOLA

SPS/14/MEE/00003

A THESIS SUBMITTED TO THE POSTGRADUATE SCHOOL OF BAYERO UNIVERSITY, KANO, IN PARTIAL FULFILLMENT OF THE REQUIREMENTS FOR THE AWARD OF MASTERS OF ENGINEERING (COMMUNICATIONS) DEGREE.

APRIL, 2019

DECLARATION

I hereby declare that I carried out the work reported in his dissertation in the Department of Electrical Engineering, Bayero University, Kano under the supervision of **Prof. M. Ajiya.** I also solemnly declare that to the best of my knowledge, no part of this dissertation has been submitted here or elsewhere in a previous application for award of a degree. All sources of knowledge used have been duly acknowledged.

……

ARANSIOLA, ISMAILA ABIOLA

SPS/14/MEE/00003

CERTIFICATION

This is to certify that the thesis titled "Minimization of Four-Wave Mixing in Wavelength Division Multiplexing Optical Communication Systems" by **Aransiola, Ismaila Abiola (SPS/14/MEE/00003),** meets the requirements and regulations governing the award of the Master of Engineering (Communication) degree of Bayero University, Kano and is approved for its contribution to knowledge and literary presentation.

Supervisor ……... **……..**
Prof. M. Ajiya **Date**

P.G. Coordinator ……... **……..**
Prof. N. Magaji **Date**

Head of Department …… **……..**
Prof. S.B. Ibrahim **Date**

External Examiner ……... **…….**

Date

APPROVAL

This dissertation has been examined and approved for the award of master in (Communication Engineering).

Thesis Supervisor……... ……..
Prof. M. Ajiya

Internal Examiner……...……..

External Examiner ……...……..

Head of Department ……...……..
Prof. S.B. Ibrahim

Board of School of Postgraduate Studies……

ACKNOWLEDGEMENT

My deepest gratitude goes to my supervisor, Professor Mohammed Ajiya for his guidance and support. I really benefited from working with him both professionally and intellectually. More importantly, I have benefited tremendously from his broad range of experience, technical insights, vision, inspiration and enthusiasm for research. In fact, I appreciate his care, patience and dedication in constructively criticizing my research work and thesis as well. Also, I would like to thank all lecturers and members of staff of the department of Electrical Engineering, Bayero University Kano for their strong academic support and encouragement that lead to the completion of this thesis. Without them it would have been a toughest time. I thank you all.

I would like to thank my senior colleague and friend. Engr. Jeleel Alao Oladapo for his support and guidance.

I would as well like to thank my colleagues, Shuaibu Alhassan Usman, Funom Benjamin Gonoh, Aminu Momoh, Bolakale Olayinka, Mubarak Isa, Yunusa Magaji and Zayanu Mustapha, for their friendship, support, and encouragement. Finally, I thank all the members of my family most especially my wife for her support, encouragement and constant love which has been my source of patience, inspiration, motivation, courage and strength.

DEDICATION

This project is dedicated to my parents, Alhaji and Alhaja Yusuf Aransiola, who gave me good background from the onset. May God continue to be with them. Ameen.

TABLE OF CONTENTS

CHAPTER THREE

METHODOLOGY

LIST OF TABLES

LIST OF FIGURES

LIST OF ABBREVIATIONS

A_{eff}	-	Effective area of optical fiber
BER	-	Bit Error Rate
B_i	-	Propagation constant of the mode is
BOF	-	Bessel Optical Filter
C	-	Speed of Light
CPM	-	Cross-Phase Modulation
CW	-	Continuous Wave
CWDM	-	Coarse Wavelength Division Multiplexing
D	-	Dispersion parameter
DCF	-	Dispersion Compensation Fiber
EM	-	Electromagnetic
F	-	Frequency
FBG	-	Fiber Bragg Grating
FWM	-	Four Wave Mixing
I	-	Intensity
IIR	-	Infinite Impulse Response
L	-	Length
LD	-	Laser Diode
LED	-	Laser Emitting Diode
L_{eff}	-	Effective Length
MUX	-	Multiplexer
n	-	Refractive index

NDSF - Non Dispersion Shifted Fiber

NRZ - Non- Return to Zero

OSA - Optical Spectrum Analyzer

OSNR - Optical Signal to Noise Ratio

P - Total Polarization, vector

P - Power

PC - Polarization Controller

P_i - Input power

SBS - Stimulated Brillouin Scattering

SMF - Single Mode Fiber

SMS - Stimulated Raman Scattering

SPM - Self Phase Modulation

SRS - Stimulated Raman Scattering

t - Time

WDM - Wavelength Division Multiplexing

$X^{(j)}$ - j^{th} order susceptibility

XPM - Cross Phase Modulation

z - Distance

α - Attenuation constant (I/m)

λ - Wavelength

ω_i - Angular frequency

ABSTRACT

The optical networks are fast, robust and error-free, but there are some nonlinearity hindrances which prevent them from being a perfect medium. The performance of wavelength division multiplexing (WDM) is found to be intensely influenced by nonlinearity characteristics within the fiber. Four-wave mixing (FWM) is a type of nonlinear effect which occurs in WDM systems when light of two or more different wavelengths are launched into a fiber. FWM causes interchannel crosstalk, intersymbolic interference, generates additional noise and degrades system performance in WDM systems. One of the objectives of this research is to simulate the FWM effect in WDM with optical components in optical simulation software called optisystem in order to minimize this nonlinear effect called FWM. Previously duobinary modulation technique was used, this research uses polarization controller, dispersion compensation fiber + fiber bragg grating, bessel optical filter, unequal channel spacing and optical infinite impulse response(optical IIR) filter techniques to minimize the FWM effect. The effect of polarization controller, the FWM effect was minimized to – 80dBm with respect to the FWM sideband and the threshold value of input power obtained was 22dBm. Effect of bessel optical filter, the FWM effect was minimized to -84dBm with respect to the FWM sideband and the threshold value of input power obtained was 27dBm. The effect of dispersion compensation fiber and fiber bragg grating, the FWM effect was minimized to -85dBm with respect to the FWM sideband and the threshold value of input power obtained was 30dBm. With the effect of unequal channel spacing, the FWM effect was minimized to -88dBm with respect to the FWM sideband and the threshold value of input power obtained was 30dBm. Finally, the effect of optical IIR filter, the FWM effect was minimized to -99dBm with respect to the FWM sideband and the threshold value of input power obtained was 40dBm. The threshold value of input power is the input power level below which the optical signal to noise ratio (OSNR) is constant. In each of these four wave mixing minimization methods employed, noise was eliminated in the WDM systems.

CHAPTER ONE

INTRODUCTION

1.1 Background

The interactions between three wavelengths produce a fourth wavelength, this phenomenon is called four-wave mixing. Four-Wave Mixing is a non-linear effect in Wavelength Division Multiplexing (WDM) systems. Four-wave mixing (FWM) is a third-order non-linear effect. It is caused by the dependence of refractive index on the intensity of the optical power.

The concept of three electromagnetic fields interacting to produce a fourth field is central to the description of all four-wave mixing processes. Physically, we may understand this process by considering the individual interactions of the fields within a dielectric medium. The first input field causes an oscillating polarization in the dielectric which re-radiates with some phase shift determined by the damping of the individual dipoles. The application of a second field will also drive the polarization of the dielectric, and the interference of the two waves will cause harmonics in the polarization at the sum and difference frequencies. Now, application of a third field will also drive the polarization, and this will beat with both the other input fields as well as the sum and difference frequencies. This beating with the sum and difference frequencies is what gives rise to the fourth field in four-wave mixing. Since each of the beat frequencies produced can also act as new source fields, a bewildering number of interactions and fields may be produced from this basic process (Schneider,T.,2013).

The phenomenon of interaction between two or more wavelengths to produce more wavelengths due to scattering of photons incident on the fiber is known as four wave mixing (FWM) also named as four photon mixing. It is one of the most crucial parameter which

determines the performance of an optical transmission system. It is observed that two or more information carrying optical signals travelling in the same fiber interact with each other very weakly. However over long-haul transmission, these weak interactions become very significant. The main reason of four wave mixing in optical fiber is the change of refractive index with optical power. Four wave mixing can also be considered as kerr effect in optical domain. Chromatic dispersion and fiber non-linear effects pose a major restriction on maximum repeater distance and bandwidth of fiber optic communication system. The interactions between information carrying optical signal and optical fiber can lead to signal interference, signal distortion, scintillations and distortion of information carrying signal which degrades system's performance. Four waves mixing is a third order distortion of signal in which two or more nearby frequency travelling in the same fiber interact with each other and as a result produce new frequencies also known as beat frequencies which travel along the original signal travelling in the fiber. As a result of FWM in a multichannel system several impairments occur in the transmission process such as crosstalk and inter symbolic interference (ISI) which degrades the overall performance of the system (Singh,M.,2015).

Four wave mixing leads to interchannel crosstalk in WDM systems. FWM generates additional noise and degrades system performance. Four wave mixing also leads to intersymbolic interference.

1.2 Motivation

The optical networks are of high speed capability and low cost, but there are some nonlinearity hindrances which prevent them from being a perfect medium. The performance of wavelength division multiplexing (WDM) is found to be greatly influenced by nonlinearity characteristics within the fibers. Four-Wave Mixing (FWM) is defined as an undesirable

nonlinear effect that causes significantly degraded system performance for optical communication systems.

In this research, the performance of WDM networks is analyzed using different techniques. The effect of input signal power on FWM is studied. Also the threshold values of input power is obtained and hence incorporation of polarization controller, bessel optical filter, dispersion compensation fiber, fiber bragg grating, unequal channel spacing, optical infinite impulse response filter are used in this research for reducing FWM effect in WDM networks.

1.3 Problem Statement

Four-wave mixing pose a major restriction on maximum repeater distance and bandwidth of fiber optic communication system. As a result of FWM in a multichannel system several impairments occur in the transmission process such as crosstalk and inter symbolic interference (ISI) which degrades the overall performance of the system.

Therefore there is need to reduce the four wave mixing sideband, eliminate noise in the channels and also obtain a higher threshold value of input power in order to minimize the four wave mixing effect in WDM optical communication systems.

Crosstalk is the power transferred from one channel to another which can occur due to the nonlinear effect, especially the FWM effect which produces crosstalk between wavelength channels. The crosstalk strongly depends on the channel separation, optical power and number of sources. “Cross-talk” is when light is scattered from one fiber optic strand to another within a jacketed fiber bundle (or light guide) consisting of several fiber optic strands. It is strongly associated with packing fraction losses. This occurs in both coherent an incoherent fiber bundles. “Cross-talk” can also occur when unwanted light from one unjacketed fiber optic strand scatters to another, when they are aligned side-by-side. This is common in

communication applications when two fibers transmitting separate signals are in close proximity. In an optical fiber, the exchange of optical power between the core and the cladding, the cladding and the environment, or layers with different refractive indexes, optical fiber crosstalk usually is undesirable because differences in path length and propagation delay usually results in dispersion, thus reducing transmission distances.

Inter symbolic interference is a signal distortion in telecommunication. One or more symbols can interfere with other symbols causing noise or a less reliable signal. The main causes of inter symbolic interference are multipath propagation or non-linear frequency in channels. This has the effect of a blur or mixture of symbols, which can reduce signal clarity. If inter symbolic interference occurs within a system, the receiver output becomes erroneous at the decision device. Therefore, both the crosstalk and ISI effect needs to be minimized so as to reduce signal distortion.

1.4 Research Aim and Objectives

The aim of this research is to minimize four wave mixing nonlinearity effect in wavelength division multiplexing optical communication systems. The objectives of this research are**:**

1. To simulate the FWM effect in WDM system using optisystem optical library components.
2. To evaluate the performance parameters associated with correction of four wave mixing effect in terms of signal power, noise power, optical signal to noise ratio (OSNR), FWM sideband and threshold value of input power.
3. To validate the results by comparing the results with existing literatures in the field.

1.5 Scope of the Work

The scope of this study is limited to simulation carried out in optisystem, optical system simulation software developed by optiwave system Inc.

1.6 Limitation of the Work

This research is limited in some areas, for instance the study is limited to analyzing the performance parameters such as signal power, noise power, optical signal to noise ratio (OSNR), four wave mixing sideband, and threshold value of input power.

1.7 Organization of the Thesis:

The first chapter presents the introductory background of four-wave mixing effect, also the problem statement, motivation, scope, aim and objectives and limitation of the project were clearly stated in this chapter. Chapter two presents the definition and explanation of nonlinear effects in optical fibers, major nonlinear effects in optical fibers, dynamics and advantages and disadvantages of each of the nonlinear effects in optical fibers, and origin of four wave mixing effect. The previous works on four wave mixing is also reviewed in this chapter. Chapter three tagged the methodology of the thesis. The research design as well as operating principle of minimization of FWM setup considered in this thesis was properly discussed in this chapter. The input and output parameters used in the minimization of four wave mixing effect in this study are also discussed in details in this chapter. Chapter four presents all the simulation results from the optisystem software. The performance analysis through performance parameter is done by presentation through Microsoft excel plotted graphs and spectrum obtained from the result of the simulation for the better understanding of the analysis. The summary result of the analysis is also contained in this chapter. Chapter five concludes the findings of this simulation research

and provides the recommendation for future studies for the further minimization of four wave mixing effect.

CHAPTER TWO

LITERATURE REVIEW

2.1 Introduction

This chapter introduces other types of modulation techniques, the concept of nonlinear effects in optical fibers and its various types. The dynamics, advantages and disadvantages of each of the nonlinear effects were also discussed. The origin of four wave mixing effect was also discussed. Previous works of FWM are also presented.

2.2 Others Types of Modulation Techniques

1. QAM modulation
2. QPSK modulation
3. DPSK modulation
4. Hybrid modulation

2.2.1 Quadrature Amplitude Modulation (QAM)

QAM is a modulation scheme used for both digital and analog signals. QAM doubles the effective bandwidth by combining two amplitude – modulated signals into a single channel. This allows multiple analog signals to be placed on a single carrier. QAM is a technique used to transmit two digital bit streams or two analog signals by modulating or changing the amplitudes of two carrier waves so that they differ in phase by 90 degrees, a quarter of a cycle, hence the name quadrature. One signal is called the "1" signal and the other is the "Q" signal, which can be mathematically represented by a cosine and a sine wave respectively. QAM combines the two carriers and sends the combined signals in a single transmission to be separated and

extracted at the destination. The signals are demodulated , and the data are then extracted from each and combined to form the original modulating information.

2.2.2 Quadrature phase shift keying(QPSK)

QPSK is a modulation technique, which actually transmits two bits per symbol. In other words, a QPSK symbol does not represent o or 1- it represents 00,01,10 or 11. This two-bits-per-symbol performance is possible because the carrier variations are not limited to two states. In ASK, for example, the carrier amplitude is either amplitude option A (representing a 1) or amplitude option B (representinga O). In QPSK, the carrier varies in terms of phase, not frequency, and there are four possible phase shifts. In a word it is a system of modulating digital signals on to a radio-frequency carrier signal using four phase 0,90,180,270 degree states to code two digital bits. QPSK is another modulation technique, and it is a particularly interesting one because it actually transmits two bits per symbol. In other words, a QPSK symbol does not represent 0 or 1- it represents 00,01,10 or 11. This two-bits-per-symbol performance is possible because the carrier variations are not limited to two states. In ASK , the carrier amplitude is either amplitude option A (representing a 1) or amplitude option B (representing a 0). In QPSK, the carrier varies in terms of phase, not frequency, and there four possible phase shifts.

2.2.3 Differential phase shift keying (DPSK)

DPSK is a common form of phase modulation that conveys data by changing the phase of the carrier wave. In phase shift keying, High state contains only one cycle but DPSK contains one and half cycle. High state is represented by a M in modulated signal and low state is represented by a wave which appears like W in modulated signal. DPSK encodes two distinct signals of same frequency with 180 degree phase difference between the two. The experiment requires two 180 degree out of phase carrier and modulating signals. Sine waveform oscillator is

selected as carrier signal. DSG converts DC input voltage into pulse trains. These pulse trains are taken as modulating signals. In actual practice modulating signal is digital form of voice or data. Sine wave is selected as carrier and 180 degree phase shift is obtained using Opamp. Different methods are used to demodulate DPSK. The analog scheme is the PLL (Phase Locked Loop). In DPSK, during HIGH state of the modulating signal fleadsignal is allowed to pass and during LOW state of the modulating signal flag signal is allowed to pass. The Opamp is tied in the inverting amplifier mode.

2.2.4 Hybrid modulation

In digital communication the three basic modulation techniques are frequency-shift keying, phase-shift keying and amplitude-shift keying. An hybrid modulation is a modulation that uses more than one of these, the most common is Quadrature amplitude modulation (QAM) where you modulate using both amplitude and phase.

2.3 Nonlinear Effects in Optical Fibers

The terms linear and nonlinear in optics mean intensity independent and intensity-dependent phenomena respectively as shown in Figure 2.1. Nonlinear effects in optical fibers occur due to:

1. Change in the refractive index of the medium with optical intensity and,

2. Inelastic scattering phenomenon.

The power dependence of the refractive index is responsible for the Kerr-effect. Depending upon the type of input signal, the Kerr-nonlinearity manifests itself in three different effects such as Self-Phase Modulation (SPM), Cross-Phase Modulation (CPM) and Four-Wave

Mixing (FWM) as shown in Figure 2.2. At high power level, the inelastic scattering phenomenon can induce stimulated effects such as Stimulated Brillouin-Scattering (SBS) and Stimulated Raman-Scattering (SRS). The intensity of scattered light grows exponentially if the incident power exceeds a certain threshold value. The difference between Brillouin and Raman scattering is that the Brillouin generated phonons (acoustic) are coherent and give rise to a macroscopic acoustic wave in the fiber, while in Raman scattering the phonons (optical) are incoherent and no macroscopic wave is generated.

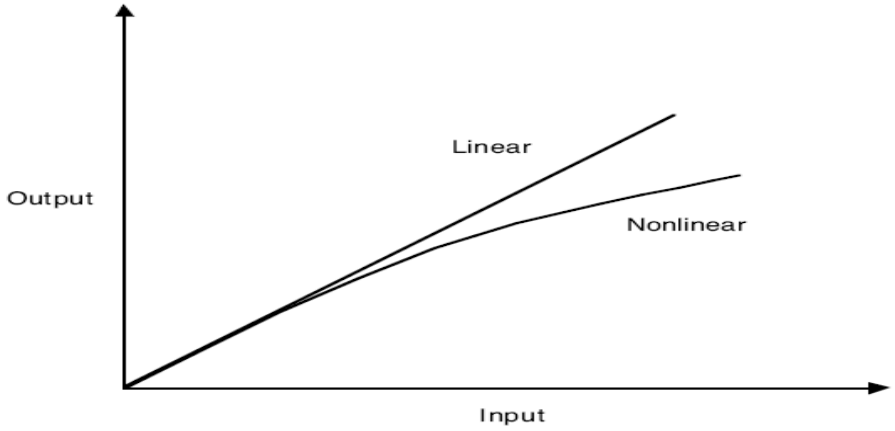

Fig. 2.1: Linear and Nonlinear Interactions.

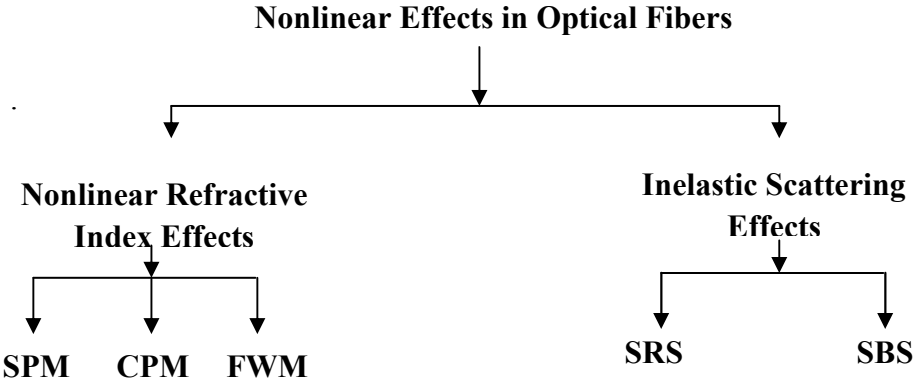

Fig. 2.2: Nonlinear Effects in Optical Fibers (Ajiya, M., 2015).

2.4 Major Nonlinear Effects

1. Stimulated Raman Scattering (SRS)
2. Stimulated Brillouin Scattering (SBS)
3. Self-Phase Modulation (SPM)
4. Cross-Phase Modulation (XPM)
5. Four-Wave Mixing (FWM)

2.4.1 Stimulated Raman Scattering

Scattering of light from vibrating silica molecules. Amorphous nature of silica turns vibrational state into a band. Raman gain spectrum extends to 41 THz. Raman gain is maximum near 13 THz. Scattered light red-shifted by 100 nm in the 1.5 μm region.

2.4.1.1 SRS Dynamics

SRS process is governed by two coupled equations:

$$\frac{dI_p}{dz} = -g_R I_p I_s - \alpha_p I_p, \frac{dI_s}{dz} = g_R I_p I_s - \alpha_s I_s. \quad (2.1)$$

If we neglect pump depletion ($I_s << I_p$), pump power decays exponentially, and the Stokes beam satisfies.

$$\frac{dI_s}{dz} = -g_R I_0 e - \alpha_{pz} I_s - \alpha_s I_s \quad (2.2)$$

This equation has the solution

$$I_s(L) = I_s(0) \exp(g_R I_0 L_{eff} - \alpha_p L),\ L_{eff} = [1 - \exp(-\alpha_p L)]/\alpha_p \quad (2.3)$$

SRS acts as an amplifier if pump wavelength is chosen suitably.

2.4.1.2 Advantages and Disadvantages of SRS

Advantages

1. Raman amplifiers are a boon for WDM systems.
2. Can be used in the entire 1300-1650 nm range
3. Erbium-doped fiber amplifiers limited to ~40 nm.
4. Distributed nature of amplification lowers noise.
5. Likely to open new transmission bands.

Disadvantages

1. Raman gain introduces interchannel crosstalk in WDM systems.
2. Crosstalk can be reduced by lowering channel powers but it limits the number of channels.

2.4.2Stimulated Brillouin Scattering

Scattering of light from acoustic waves. Becomes a stimulated process when input power exceeds a threshold level. Low threshold power for long fibers (~5 mW)

2.4.2.1Brillouin Shift

Pump produces density variations through electrostriction, resulting in an index grating which generates Stokes wave through Bragg diffraction. Energy and momentum conservation require :

$$\Omega_B = \omega_p - \omega_s \overrightarrow{k_A} = \overrightarrow{k_p} - \overrightarrow{k_s} \quad (2.4)$$

Acoustic waves satisfy the dispersion relation:

$$\Omega_B = V_A/\overrightarrow{k_A}/ \approx 2V_A/\overrightarrow{k_p}/\sin(\theta/2) \quad (2.5)$$

In a single- mode fiber $\Theta = 180^0$, resulting in

$$v_B = \Omega_B/2\pi = 2n_p v_A/\lambda_p \approx 11\ GH_z \quad (2.6)$$

Where n_p is the fiber refractive index of the medium.

V_A is the speed of the sound in the medium and λ_p is the pump wavelength.

If we use $V_A = 5.96 km/s, n_p = 1.45, and \lambda_p = 1.55\ \mu m,$ the value appropriate Brillouin shift for silica fibers is $v_B \approx 11\ GH_z$

2.4.2.2Brillouin Threshold

Pump and Stokes along the fiber as

$$-\frac{dI_s}{dz} = -g_B I_p I_s - \alpha I_s, \quad \frac{dI_p}{dz} = -g_B I_p I_s - \alpha I_p. \quad (2.7)$$

Ignoring pump depletion, $I_p(z) = I_0\exp(-\alpha z)$.

Solution of the Stokes equation;

$$I_s(L) = I_s(0)exp(g_B I_o L_{eff} - \alpha L). \quad (2.8)$$

Brillouin threshold is obtained from

$$\frac{g_B P_{th} L_{eff}}{A_{eff}} \approx 21 \rightarrow P_{th} \approx \frac{21 A_{eff}}{g_B L_{eff}} \quad (2.9)$$

Brillouin gain $g_B \approx 5 \times 10^{-11} m/W$ is nearly independent of the pump wavelength.

2.4.3 Self-Phase Modulation

Refractive index depends on optical intensity as

$$n(\omega, I) = n_0(\omega) + n_2 I(t). \tag{2.10}$$

Leads to nonlinear Phase shift

$$\emptyset_{NL}(t) = (2\pi/\lambda) n_2 I(t) L. \tag{2.11}$$

An optical field modifies its own phase (SPM). Phase shift varies with time for pulses. Each optical pulse becomes chirped. As pulse propagates along the fiber, its spectrum changes because of SPM.

2.4.3.1 Advantages and Disadvantages of SPM

Advantages

1. Modulation instability can be used to produce ultra short pulses at high repetition rates.
2. SPM can be used for fast optical switching.
3. It has been used for passive mode locking.
4. Responsible for the formation of optical solitons.

Disadvantages

1. SPM-induced spectral broadening can degrade performance of a light wave system.
2. Modulation instability often enhances system noise.

2.4.4 Cross-Phase Modulation

Consider two optical fields propagating simultaneously. Nonlinear refractive index seen by one wave depends on the intensity of the other wave as

$$\Delta n_{NL} = n_2 (|A_1|^2 + b|A_2|^2). \tag{2.12}$$

Nonlinear phase shift:

$$\emptyset_{NL} = (2\pi L/\lambda) n_2 [I_1(t) + bI_2(t)]. \quad (2.13)$$

An optical beam modifies not only its own phase but also of other copropagating beams (XPM).

XPM induces nonlinear coupling among overlapping optical pulses.

2.4.4.1 Advantages and Disadvantages of CPM

Advantages

1. Nonlinear Pulse Compression.
2. Passive mode locking.
3. Ultrafast optical switching.
4. Demultiplexing of OTDM channels.
5. Wavelength conversion of WDM channels.

Disadvantages

1. XPM leads to interchannel crosstalk in WDM systems.
2. It can produce amplitude and timing jitter.

2.5 Four-Wave Mixing (FWM)

Degenerate four-wave mixing- Four-wave mixing is also referred to as degenerate four-wave mixing when there are three components involved and all the waves have the same frequency. Non-degenerate FWM- is also present, if only two components interact as shown Figure 2.3.

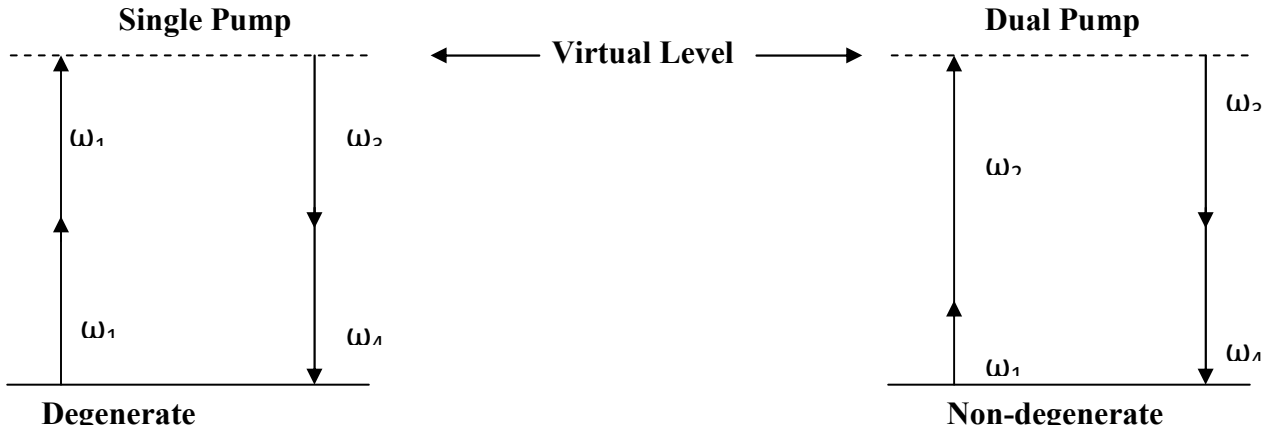

Fig. 2.3: Four-Wave Mixing

FWM is a nonlinear process that transfers energy of pumps to signal and idler waves. FWM requires conservation of

(notation: $E = Re\,[A\exp(i\beta z - i\omega t)]$) (2.14)

Energy $\omega_1 + \omega_2 = \omega_3 + \omega_4$

Momentum $\beta_1 + \beta_2 = \beta_3 + \beta_4$

Degenerate FWM: Single pump $(\omega_1 = \omega_2)$.

2.5.1 Disadvantages of FWM

Disadvantages

1. FWM leads to interchannel crosstalk in WDM systems.
2. FWM generates additional noise and degrades system performance.
3. FWM leads to intersymbolic interference.

Self-Phase Modulation (SPM), Cross-Phase Modulation (CPM) and Four-Wave Mixing (FWM) are nonlinear effects in optical fibers that occur due to change in the refractive index of the medium with optical intensity and their comparison is shown in Table 2.1.

Table 2.1: Comparison of Nonlinear Refractive Effects.

Nonlinear Phenomenon → / Characteristics ↓	**SPM**	**CPM**	**FWM**
1. Bit-rate	Dependent	Dependent	Independent
2. Origin	Nonlinear susceptibility $\chi^{(3)}$	Nonlinear susceptibility $\chi^{(3)}$	Nonlinear susceptibility $\chi^{(3)}$
3. Effects of $\chi^{(3)}$	Phase shift due to pulse itself only	Phase shift is alone due to copropagating signals	New waves are generated
4. Shape of broadening	Symmetrical	May be a symmetrical	-
5. Energy transfer between medium and optical pulse	No	No	No
6. Channel spacing	No effect	Increases on decreasing the spacing	Increases on decreasing the spacing

2.6 Origin of Four-Wave Mixing

The origin of FWM process lies in the nonlinear response of bound electrons of a material to an applied optical field. In fact, the polarization induced in the medium contains not only linear terms but also the nonlinear terms. The magnitude of these terms is governed by the nonlinear susceptibilities of different orders. The FWM process originates from third order nonlinear susceptibility. If three optical fields with carrier frequencies ω_1, ω_2 and ω_3, copropagate inside the fiber simultaneously, susceptibility generates a fourth field with frequency ω_4, which is related to other frequencies by a relation, $\omega_4 = \omega_1 \pm \omega_2 \pm \omega_3$. In quantum-mechanical context, FWM occurs when photons from one or more waves are annihilated and new photons are created at different frequencies such that net energy and momentum are conserved during the interaction. Self-Phase Modulation (SPM) and Cross Phase Modulation (CPM) are significant mainly for high bit rate systems, but the FWM effect is independent of the bit rate and is critically dependent on the channel spacing and fiber dispersion. Decreasing the channel spacing increases the four-wave mixing effect and so does decreasing the dispersion(Singh,S.P.,2007).

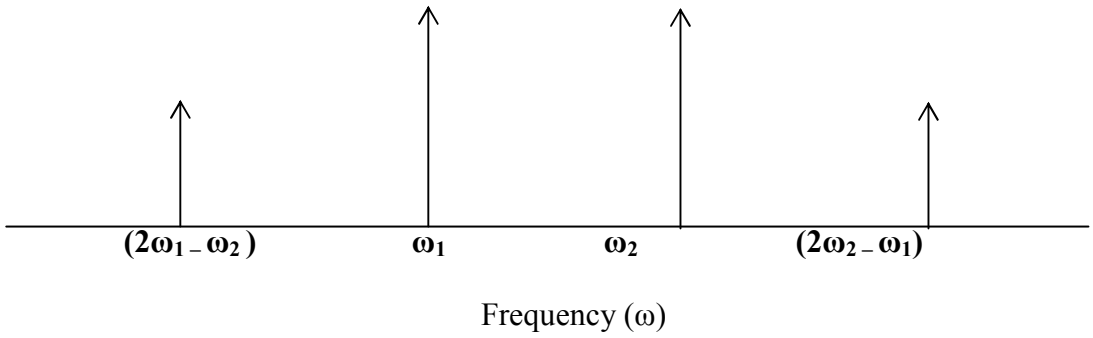

Fig. 2.4: Showing mixing of Two Waves.

Figure 2.4 shows a simple example of mixing of two waves at frequency ω_1 and ω_2. When these waves mixed up, they generate sidebands at $(2\omega_1-\omega_2)$ and $(2\omega_2 -\omega_1)$. Similarly, three copropagating waves will create nine new optical sideband waves at certain frequencies. These sidebands travel along with original waves and will grow at the expense of signal-strength depletion. In general for N-wavelengths launched into fiber, the number of generated mixed products M is,

$$M = N^2/ 2. (N-1) \quad (2.15)$$

2.7 Previous Works on FWM

A lot of works have been reported on four-wave mixing, for instance (Saurabh Kothari et al., 2014) showed that the FWM decreases with the increase of the channel spacing of transmitted signals, dispersion and core effective area of the fiber. The four wave mixing side band obtained was -40dBm. This sideband is high. The reason for this high sideband is due to the absence of a filter. The result obtained shows that the FWM decreases with the increase of the channel spacing of transmitted signals, dispersion and core effective area of the fiber [1].

A. Panda and D.P. Mishra, 2014 showed that the magnitude of FWM depends on channel power, channel spacing and fiber dispersion but is independent of the bit rate. The four mixing sideband obtained was -38dBm. This sideband is high. The reason for this high sid3eband is because of the absence of polarization controller. The information capacity of a light wave is ultimately limited by the nonlinear interactions between the information signals and the fiber medium [2].

Mehtab Singh and Vishal Sharma, 2015 showed that as the transmission power is increased, the efficiency of four wave mixing effect increases. Also if the channel spacing in a WDM system is kept uneven, the power levels of mix frequencies produced as a result of FWM effects is

reduced to a considerable amount. The FWM sideband obtained was -50dBm. This sideband is high. The reason for this high sideband is because of the absence of dispersion compensation fiber. Analysis of effect of increasing optical transmission powers and channels spacing in a wavelength division multiplexing system was done [3].

Veerpal Kaur and Kamaljit Singh Bhatia, 2015 investigated the effect of channel spacing and chromatic dispersion on four wave mixing in WDM system and that dominating effect of four vgwave mixing is minimizing at maximum value of dispersion and channel spacing. Power of FWM, Q-factor, bit error rate and output spectrum were used to measure the performance of the system. The FWM sideband obtained was -67dBm. The FWM can be minimized here by the incorporation of fiber bragg grating. This result shows that increasing chromatic dispersion and channel spacing, decreases the FWM [4].

Surbhi Jain and A. Brintha Therese, 2015 analyzed the performance of WDM network using optical filter (rectangle filter) and various external modulation schemes under FWM nonlinearity effect. Here, the effect of input signal power on FWM was studied. The FWM sideband obtained -69.6dBm. This sideband is slightly high. The reason for this, is because of the absence of polarization controller, bessel optical filter, dispersion compensation fiber + fiber bragging grating and optical IIR filter. Duobinary modulation is found to be the optimal technique for reducing FWM effect [5].

Haider Jabber Abed, N.M. Din et al., 2014 presents a method to suppress the FWM through system parameters optimization. The study was conducted on four different types of optical fiber, i.e. Single- Mode Fiber (SMF), Dispersion Shifted Fiber (DSF), Non-zero Dispersion Fiber (NZDF) and Non-zero Dispersion Shifted Fiber (NZDSF). The results proved that the optimization of the parameters can reduce the effect of FWM in optical fiber link. It showed that a maximum FWM power level was observed with DSF and a minimum FWM power level with

SMF with little effect on the optical link channel. The FWM sideband obtained was -45dBm. This sideband is high. The reason for this sideband is because of the absence of dispersion compensation fiber and fiber bragg grating in this work. This result proved that the optimization of the parameters can reduce the effect of FMW in optical fiber link [6].

Deven Bhalla and Monica Bhutani, 2014 discussed the effect of channel spacing, laser power and dispersion, length of the optical fiber and the variation of input power to compensate the effect of FWM when implemented in a short haul environment. The FWM sideband obtained was -47dBm. This sideband is high. The reason for this is due to the absence of polarization controller or dispersion compensation fiber + fiber bragg grating. FMW effect is resonant when the phase matching condition is satisfied. It only occurs for particular combinations of fiber dispersion and signal frequencies [7].

S. Esther Jenifer , K. Gokulakrishnan, 2014 showed that Hybrid Modulator technique, Return to Zero (RZ) pulse generator and Dispersion Compensation Fiber (DCF) have proposed to reduce the Four Wave Mixing (FWM) in equal channel spacing. The single and combined effect of various parameters such as input power, effective area, channel spacing and fiber length were analyzed to determine the effect of FWM power. The result showed that increasing sequentially the effective area, fiber length, channel spacing and decreasing the input power can suppress the FWM effect. The noise power obtained was -60.12dBm and the FMW sideband obtained was -49dBm. Both the noise power and the FMW sideband are slightly high. This is due to the absence of filter, fiber bragg grating and lack of the use of unequal channel spacing in this work. The single and combined effect of various parameters such as input powers, effective area, channel spacing and fiber length have been analyzed to determine the effect of FWM[8].

A. Panda and D.P. Mishra, 2013 investigated the FWM effect with different number of channels at various channel spacing. The FWM sideband obtained was -35dBm. This sideband is high.

The reason for this is due to the absence of filter, polarization controller and dispersion compensation fiber + fiber bragg grating[9].

S. Sugumaran, Sadhana Priya Vashisht et al., 2011 numerical analysis of the nonlinear effects is done by nonlinear Schrodinger equation. The equation was solved using an algorithm called split-step algorithm coded in matlab. The analysis shows that FWM is independent of bit rate but depends on fiber dispersion and channel spacing The FWM sideband obtained was -77dBm. This result can be proved upon by the incorporation of polarization controller, bessel optical filter, dispersion compensation fiber + fiber bragg grating, use of unequal channel spacing, or by the use of optial IIR filter. Thus WDM systems upgrade channel capacity, transparency and enhances wavelength switching and routing[10].

Mohammed Ali K.N, 2013 showed that FWM effects have become significant at high optical power levels and have become even more significant when the capacity of the optical transmission line is increased, which has been done by either increasing the channel bit rate, and decreasing the channel spacing, or by the combination of both process. The FWM sideband obtained was -38dBm. This sideband is high. This is due to the absence of filters, polarization controller and dispersion compensation fiber + fiber bragg grating. The FWM effects have become significant at high optical power levels and have become even more significant when the capacity of the optical transmission line is increased [11].

Rupinder Kaur, Sanjeev Dewra,2014 showed that duobinary modulation is a more efficient format for transmitting high speed optical signals over bandwidth limited channel and that the duobinary modulation format for long haul and WDM transmission links is the one that has a narrow spectral width , low susceptibility to fiber nonlinearity, large dispersion tolerance and good transmission performance and has a simple and cost-effective configuration [12].

Habib Ullah Manzoor, Abaid Ullah Salfi et al. , 2015 introduced a method in which alternative circular polarizers were used to change the polarization of input pulses into right and left handed polarized pulses before multiplexer which resulted in reduction of FWM. The FWM sideband obtained was -65dBm. This sideband is slightly high. The reason for this, is because of the absence of filters and fiber bragg grating in the setup. With the help of this technique, FWM can be minimized by optimizing optical network parameters [13].

Ishita Tiwari, Shreya Garg et al., 2015 simulated Wavelength Division Multiplexed (WDM) optical transmission system with different modulation schemes that can help in enhancing the system performance by dampening the nonlinearity effect – Four Wave Mixing (FWM). The analysis of WDM was carried out for Carrier Suppressed Return to Zero (CSRZ), Duobinary and Differential Phase Shift Keying (DPSK) modulation formats. The effect of variation in system length, dispersion and bit rate was observed in terms of Q-value and BER. Variation in output FWM power was also observed in terms of channel spacing and dispersion. It was observed that Duobinary is the optimal technique to reduce the effect of FWM. The FWM sideband obtained was -63dBm. This is slightly high. The reason for this is because of the absence of dispersion compensation fiber and fiber bragg grating in the simulation setup. FWM have vital deleterious effects in the system where it can cause cross talk between different wavelength channels and/or an imbalance in channel power [14].

Narinder Singh, Ashok K. Goel, 2016 compared Four Wave Mixing (FWM) effect on two channels Wavelength Division Multiplexing (WDM) optical communication system for different values of channel spacing. The effect of variation in input power of laser array was also been investigated. The effect of dispersion was also being considered in the optical spam of fiber and pre-dispersion compensation technique was been employed to mitigate its effect. The performance of optical communication system was been evaluated in terms of Q-factor, Bit

Error Rate (BER) and output from the Optical Spectrum Analyzer. It was simulated that the FWM effect decreases as the channel spacing increases. The FWM sideband obtained was -80dBm. This sideband is low, but can still be minimized by the use of polarization controller, filters such as bessel optical filter and optical IIR filter and also be the incorporation of fiber bragg grating [16].

Fatemah Dehghani, Farzin Emami, 2016 investigated a new approach for suppressing the four-wave mixing (FWM) crosstalk by using the pairing combinations of differently linear-polarized optical signals. The simulation was conducted using a two-channel system. The proposed technique was to suppress the FWM interaction using different input powers. It was been evaluated for single-mode fiber (SMF). The FWM sideband obtained was -81dBm. This sideband is low, but can be improved upon by the use of dispersion compensation fiber and fiber bragg grating and also by the incorporation of filters [15].

A.M. Chadha, et al., 2017, explained the most important linear and nonlinear impairments of an optical fiber and the effects of the interplay between them. The mathematical analysis of these impairments were also reviewed to obtain a better idea of the behavior of the fiber in their presence. An optical system was also simulated and observed its performance by variation in parameters such as channel spacing and dispersion. The FWM sideband obtained was -83dBm. This sideband is low, but can be minimized by the use of unequal channel spacing and also by the incorporation of optical IIR filter, bessel optical filter, dispersion compensation fiber + fiber bragg grating, or by the use of polarization controller [18].

Jaspreet Kaur, Dr. Hardeep Singh, 2017, accentuated on the emergence of four wave mixing in WDM system at different distances and to study behavior of the system for different WDM channels, frequency spacings, different optical fibers such as single mode fiber and dispersion compensation fiber, SMF effective areas. Performance of the proposed system is evaluated in

terms of Q-factor, BER and FWM is analyzed at different distances. The FWM sideband obtained was -82dBm. This sideband is low, but can still be improved upon by the use of fiber bragg grating, filters and polarization controller [17].

In order to show the improvement of this research over exiting works, the achievement and limitations of the previous works needs to be marked out. This is summarized as shown in Table 2.2.

Table 2.2: Summary of Previous Works Reviewed.

S/N	Author Name and Year	FWM Minimization Method	Performance Parameters	Limitations
1.	Kothari et al., 2014.	Increased channel spacing of transmitted signals, pure effective area and dispersion of fiber.	Sideband (SB): -40dBm. Signal Power (SP): Noise Power (NP): Optical Signal to Noise Ratio OSNR: 62dB. Threshold Value of input power (TVIP): 10dBm.	High sideband and low threshold value of input power.
2.	Din et al., 2014.	System parameters optimization.	Sideband: -45dBm. Signal Power: -6.65dBm. Noise Power: -65.21dBm. OSNR: 62.5dB. Threshold value of input power: 10dBm.	High sideband, large noise power and low threshold value of input power.
3.	Singh and Sharma, 2015.	Unequal channel spacing.	Sideband: -50dBm. Signal Power: -6.70dBm. Noise Power: -67.69dBm. OSNR: 63.5dB. Threshold value of input power: 11dBm.	High sideband, large noise power and low threshold value of input power.
4.	Kaur and Bhatia, 2015.	Increased chromatic dispersion and channel spacing.	Sideband: -67dBm. Signal Power: -6. 95dBm. Noise Power: -69.87dBm. OSNR: 65.02dB. Threshold value of input power: 12dBm.	High sideband, large noise power and low threshold value of input power.
5.	Jain and Therese, 2015.	Rectangle filter and external modulation scheme.	Sideband: -69.6dBm. Signal Power: -7.74dBm. Noise Power: -80.83dBm. OSNR: 73.08dB. Threshold value of input power: 12dBm.	High sideband, large noise power strong OSNR and low threshold value of input power.

6.	Jenifer and Gokulakrishnan, 2015.	Hybrid modulator technique dispersion compensation fiber (DCF).	Sideband: -49dBm. Signal Power: -6.65dBm. Noise Power: -60.12dBm. OSNR: 63dB. Threshold value of input power: 11dBm.	High sideband, large noise power and low threshold value of input power.
7.	Sugumaran et al., 2011.	Numerical analysis using nonlinear schrödinger equation	Sideband: -35dBm. Signal Power: Noise Power: OSNR: 62.1dB. Threshold value of input power: 10dBm.	High sideband and low threshold value of input power.
8.	Ali, 2013.	Increased channel bit rate and decreased channel spacing .	Sideband: -38dBm. Signal Power: -6.50dBm. Noise Power: -58.69dBm. OSNR: 62.3dB. Threshold value of input power: 10dBm.	High sideband, large noise power and low threshold value of input power.
9.	Singh and Goel, 2016.	Increased channel spacing.	.	Low sideband, small noise power, strong optical signal to noise ratio and low threshold value of input power.
10.	Dehghani and Emami, 2016.	Linear polarized optical signals.	Sideband: -81dBm. Signal Power: -8.12dBm. Noise Power: -74.69dBm. OSNR: 70dB. Threshold value of input power: 21dBm.	Low sideband, small noise power, strong OSNR and high threshold value of input power.
11.	Chadha et al., 2017.	Increased channel spacing and dispersion.	Sideband: -83dBm. Signal Power: -15.40dBm. Noise Power: -84.43dBm. OSNR: 67dB. Threshold value of input power: 20dBm.	Low sideband, small noise powers and low threshold value of input power.
12.	Kaur and Singh, 2017.	Dispersion compensation fiber.	Sideband: -82dBm. Signal Power: -18.40dBm. Noise Power: -98.01dBm. OSNR: 64dB. Threshold value of input power: 20dBm.	Low sideband, small noise power and low threshold value of input power.

Summary

Therefore, in most of the previous works reviewed, there are limitations specifically, high four-wave mixing sideband, large noise power and low threshold value of input power as can be clearly seen in Table 2.2 and these performance parameters need to be improved in order to minimize the FWM effect in WDM optical communication systems. Therefore in this research, duobinary modulation with incorporation of polarization controller, bessel optical filter, dispersion compensation fiber and fiber bragg grating, unequal channel spacing, and optical infinite impulse response (optical IIR) filter is used to reduce the FWM sideband, the noise power and to obtain a higher threshold value of input power in order to minimize the FWM effect in WDM optical communication systems.

CHAPTER THREE

METHODOLOGY

3.1 Introduction

This chapter presents the methodology of this research. The experimental setup and principle of operation of duobinary modulation configuration employed in this research were discussed in details. Lastly, minimization of FWM parameters under study (design parameters and performance parameters) were explained in order to have a better understanding of the research.

3.2 Principle of Operation of the Simulation Set Up

The simulation set-up consists of a sine wave generator, duobinary pulse generator, pseudo-random bit sequence generator, continuous wave laser, mach-zehnder modulator, WDM multiplexer, optical fiber CWDM, Polarization Controller (PC), Bessel Optical Filter (BOF), Dispersion Compensation Fiber (DCF), Fiber Bragg Grating (FBG), optical infinite impulse response (optical IIR) filter, optical spectrum analyzer, WDM analyzer, and optical power meter. The setup consists of signals with sine wave generator in analog form and the random bit sequence in digital form. The sine wave generator generates an electrical sine waveform signal. It excellently generates the waves. It allows both frequency and amplitude of the sine wave output to be varied. Both fine and coarse frequency control are included. The pseudorandom bit sequence generator generates a stream of O's and 1's at a rate of 2.5Gbps.

The duobinary pulse generator functions to combine both sine wave and bit sequence. The duobinary pulse generator convert the sine analog waveform into binary pulse and also converts these O's and I's in form of electric pulses having duobinary format. These electrical pulses from output of duobinary pulse generator are directed to input of mach-zehnder modulator which modulates information with a continuous wave (CW) laser. The CW laser

produces the light. Laser is a device that emits light through a process of optical amplification. The mach-zehnder modulator also function for the balancing of optical paths (optical power output) of light produced by CW laser. The setup consists of two such channels separated at some frequency interval. These two WDM channels are multiplexed and directed into an optical fiber of length 25km. The optical signal from the output of the optical fiber is directed to filter which eliminates all the high frequency noise present in the received electrical signal. At the last stage, the received signal is analyzed using optical spectrum analyzer and WDM analyzer. The block diagram of this setup is shown in Figure 3.1, where the filters (BOF, Optical IIR), PC, DCF + FBG and UCS are the correction of four-wave mixing compensators. The optisystem simulation setup is shown in Figure 3.2, were each WDM channel comprises of a sine-wave generator, pseudorandom bit sequence generator, CW laser, duobinary pulse generator and a mach-zehnder modulator.

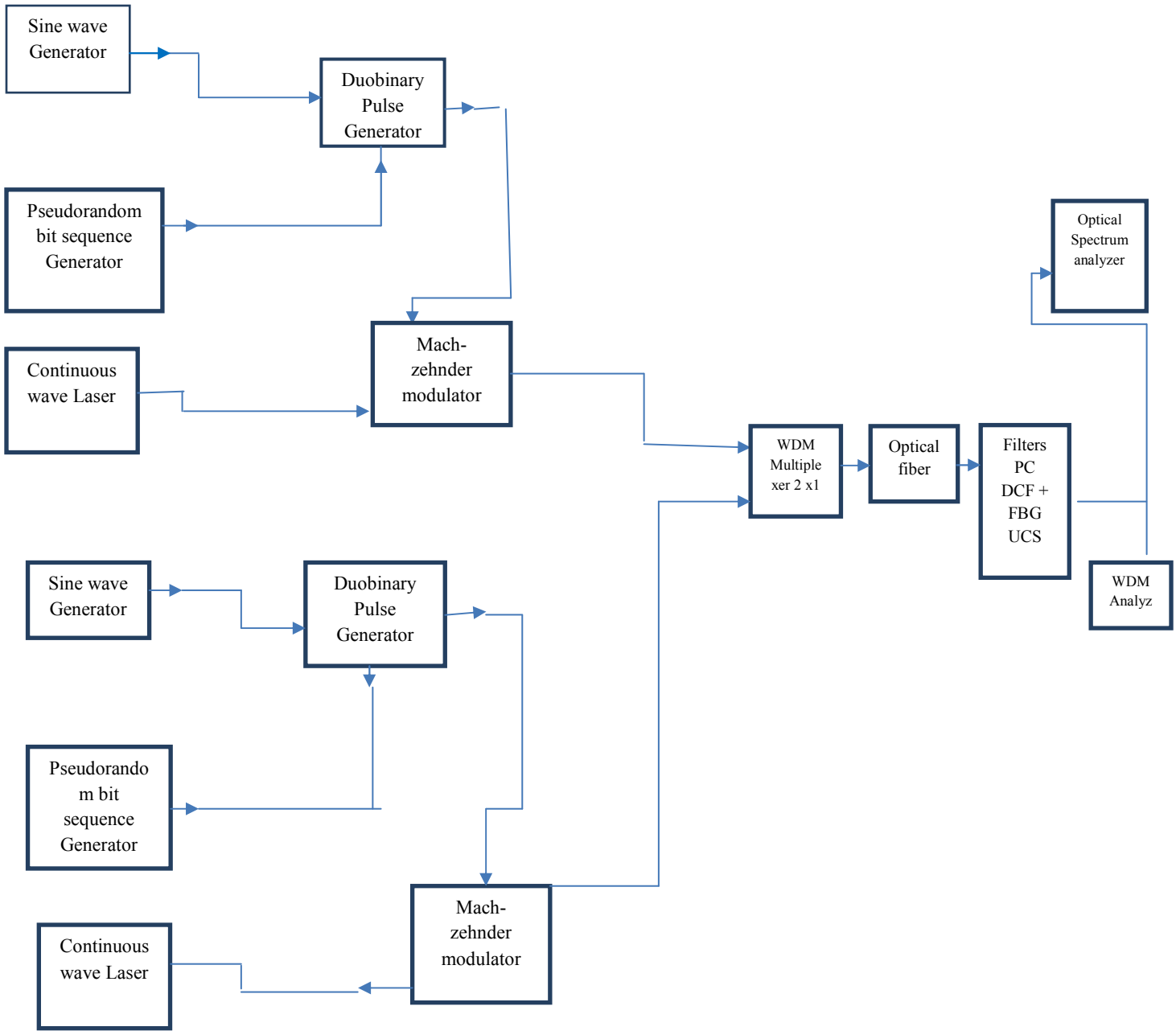

Fig.3.1 Block diagram of setup.

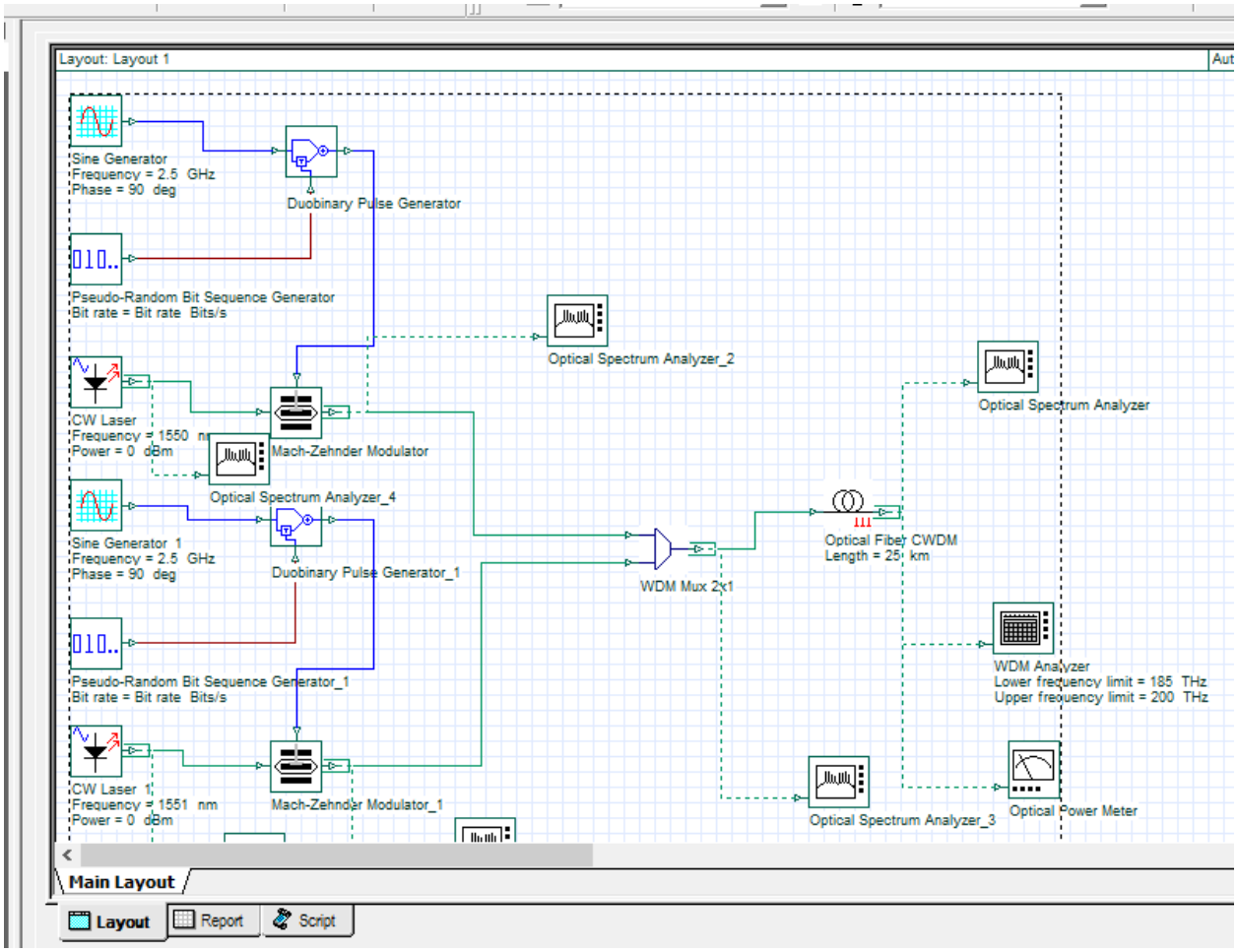

Fig. 3.2: FWM Simulation Set Up in Optisystem.

3.3 Optisystem Library Components Used in Minimization of FWM Design

The components used in this research includes sine wave generator, duobinary pulse generator, pseudorandom bit sequence generator, continuous wave laser, mach-zehnder modulator, polarization controller, Bessel optical filter, dispersion compensation fiber, fiber bragg grating, optical infinite impulse response filter, optical fiber CWDM, WDM multiplexer, optical spectrum analyzer(OSA), optical power meter, WDM analyzer. All the components used here are picked from the components library of optisystem software. The details of the components are individually discussed here.

3.3.1 Sine wave Generator

The sine wave generator is a type of electronic equipment that generates an oscillating frequency in a sinusoidal pattern. There are a couple of different reasons why the sine generator is important, but most have to do with measuring either sound or electric frequency, both of which typically take on a sine pattern. In this research the sine generator generates an electrical sine waveform signal. Sine wave generator is an excellent tool for generating waves. It allows both frequency and amplitude of the sine wave output to be varied. Both fine and coarse frequency control are included. It masters the fundamental frequency for a particular configuration.

3.3.2 Duobinary Pulse Generator

The Duobinary pulse generator is used for duobinary modulation schemes. It is equivalent to a subsystem based on an electrical delay and adder. It can be used together with any electrical pulse generator. The duobinary pulse generator is used to generate the duobinary sequence which will then be further modulated using the mach-zehnder modulator as shown in Figure 3.3.

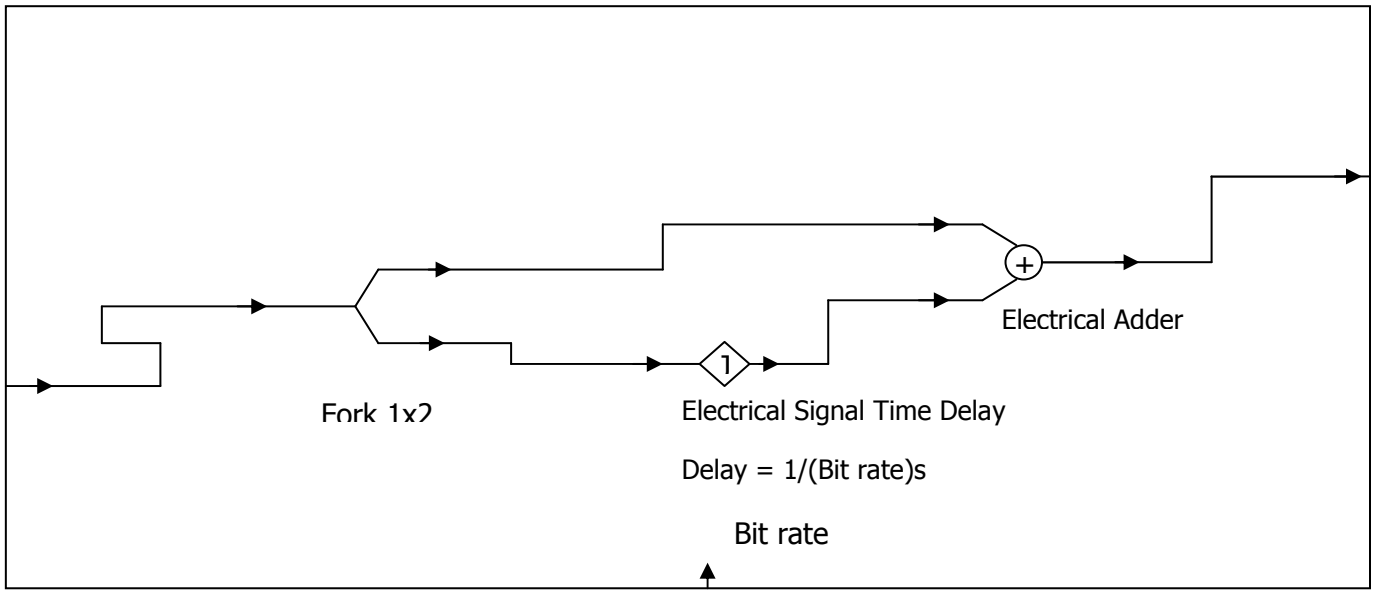

`Fig. 3.3: Duobinary Pulse Generator Subsystem (OPTIWAVE, version 13, 2014).

3.3.3 Pseudorandom Bit Sequence Generator

Pseudo-random data generator has three properties that reflect the data's randomness. Firstly, the number of marks and spaces (or "0s" and "1s") in a sequence differ by 1. Secondly, the probability of a continuous string of marks or spaces is inversely proportional to the length of the string. This means that among the number of runs of marks of spaces in the pseudo-random binary sequence (PRBS), one-half the funds of each kind are of length one, one-fourth are length two, one-eighth are length three and so on. At last, the autocorrelation of the pseudo random binary sequence is approximately zero everywhere except at the origin. The production of a pseudo random binary sequence is implemented by using a shift register with feedback has three properties that reflect the data's randomness. The pseudorandom bit sequence generator generates a sequence of N bits, where

$$N = T_W B_r, \tag{3.1}$$

$$N_G = N - n_l - n_t \tag{3.2}$$

Where T_W is the global parameter time window and B_r is the parameter Bit rate. The number of bits generated in $N_G$and n_l and n_t are the number of leading zeros and the number of trailing zeros respectively (Flannery, B., 2003).

In this research th6e pseudo random bit sequence generator generates a pseudo random binary sequence (PRBS) according to different operation modes. The operation modes controls the algorithm used to generate the bit sequence. The bit sequence is designed to approximate the characteristics of random data.

3.3.4 Mach-Zehnder Modulator

The Mach-Zehnder modulator is an intensity modulator based on an interferometric principle. It consists of two 3 dB couplers which are connected by two waveguides of equal length. By means of an electro-optic effect, an externally applied voltage can be used to vary the refractive indices in the waveguides branches. The different paths can lead to constructive and destructive interference at the output, depending on the applied voltage. Then the output intensity can be modulated according to the voltage as shown in Figure 3.4.

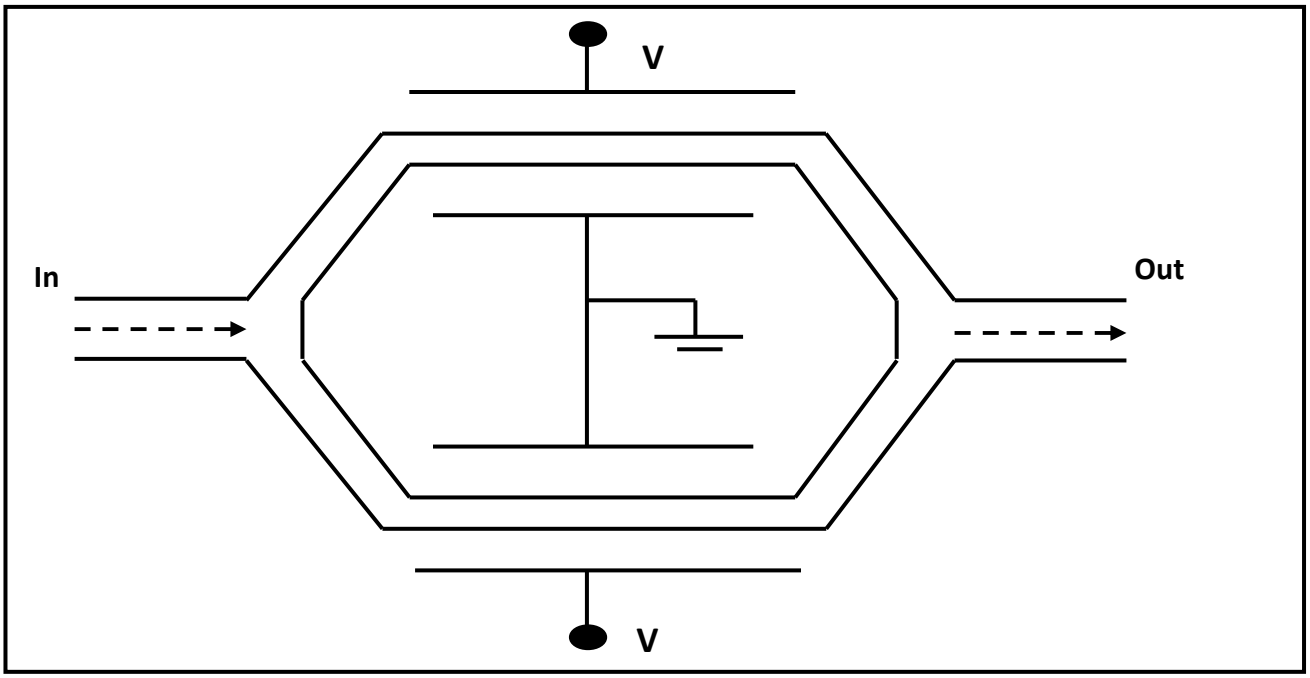

Fig. 3.4: Mach-Zehnder Modulator (OPTIWAVE, version 13, 2014).

3.3.5 Continuous Wave Laser

Lasers are used for converting electrical current into light. Laser is commonly used in optical communication because it has several advantages. Some important features of the CW laser includes small size, long life and can be modulated easily. Light emitting diode (LED) is also useful but laser has the following advantages on LED diodes. The speed of laser is faster

and provides high bandwidth and also spectral width provided by the laser is narrow as compared to LED. In this research the CW laser generates a continuous wave optical signal.

3.3.6 Polarization Controller

The polarization controller is a device which allows one to control the state of polarization of light within the fiber (core). The polarization controller sets the input signal in an arbitrary polarization state. The azimuth and ellipticity parameters define the polarization state of the output signal. In this case, the output polarization is independent of the input signal polarization.

3.3.7 Bessel Optical Filter

Bessel optical filter is an optical filter with a Bessel frequency transfer function. Bessel filters have a transfer function of the form (Agrawal,2011):

$$H(s) = \alpha \frac{d_0}{B_N(s)} \tag{3.3}$$

α is the parameter Insertion loss, N is the parameter Order, and

$$d_0 = \frac{(2N)!}{2^N . N!} \tag{3.4}$$

is a normalizing constant and $B_N(s)$ is an nth-order Bessel polynomial of the form

$$B_N(s) = \sum_{k=0}^{N} d_k S^k \tag{3.5}$$

Where $d_k = \frac{(2N-k)!}{2^{N-k} . k!(N-k)!}$

$$H(s) = \alpha \frac{d_0}{B_N(s)} \tag{3.6}$$

$$d_0 = \frac{(2N)!}{2^N . N!}$$

$$B_N(s) = \sum_{k=0}^{N} d_k S^k$$

:. H(s) =α $\left(\frac{\frac{(2N)}{2^N . N!}}{\sum_{k=0}^{N} d_k S^k} \right)$

H(s) =α $\left(\frac{\frac{2 . N!}{2^N . N!}}{\sum_{k=0}^{N} d_k S^k} \right)$

H(s) =α $\left(\frac{\frac{2!}{2^N}}{\sum_{k=0}^{N} d_k S^k} \right)$

H(s) =α $\left(\frac{\frac{(2x1)}{2^N}}{\sum_{k=0}^{N} d_k S^k} \right)$

H(s) =α $\left(\frac{\frac{2^1}{2^N}}{\sum_{k=0}^{N} d_k S^k} \right)$

H(s) =α $\left(\frac{2^{1-N}}{\sum_{k=0}^{N} d_k S^k} \right)$

N =1

H(s) = α $\left(\frac{2^{1-1}}{\sum_{k=0}^{1} d_k S^k} \right)$

H(s) =α $\left(\frac{2^0}{\sum_{k=0}^{1} d_k S^k} \right)$

H(s) =α $\left(\frac{1}{\sum_{k=0}^{1} d_k S^k} \right)$

H(s) =α $\left(\frac{1}{d_0 S^0 + d_1 S^1} \right)$

$$H(s) = \alpha \left(\frac{1}{d_0 + d_1 S} \right)$$

$$d_k = \frac{(2N-k)!}{2^{N-k}.\ k!\,(N-k)!}$$

At k = 0

$$d_0 = \frac{(2x1-0)!}{2^{1-0}.\ 0!(1-0)!}$$

$$d_0 = \frac{(2-0)!}{2^1\ \ 1(1)!}$$

$$d_0 = \frac{2!}{2x1x1!}$$

$$d_0 = \frac{2x1}{2x1x1}$$

$$d_0 = \frac{2}{2} = 1$$

At k = 1

$$d_1 = \frac{(2x1-1)!}{2^{1-1}.\ 1!(1-1)!}$$

$$d_1 = \frac{(2-1)!}{2^0.1!(0)!}$$

$$d_1 = \frac{1!}{1x1x1}$$

$$d_1 = \frac{1x1}{1x1x1}$$

$$d_1 = \frac{1}{1} = 1$$

$$H(s) = \alpha \left(\frac{1}{d_0 + d_1 S} \right)$$

$$\therefore H(s) = \alpha \left(\frac{1}{1 + (1 \times S)} \right)$$

$$H(s) = \alpha \left(\frac{1}{1+S} \right)$$

$$H(s) = \alpha \left(\frac{1}{S+1} \right) \qquad (3.7)$$

The transfer function of first order bessel optical filter is a rational function whose denominator is a reverse bessel polynomial, such $H(s) = \frac{1}{s+1}$ and this has been derived above.

And $$s = j\left(\frac{2(f - f_c).W_b}{B}\right) \qquad (3.8)$$

Where f_c is the filter center frequency defined by the parameter frequency, B is the parameter Bandwidth, and W_b denotes the normalized 3 dB bandwidth.

Where f = 1553nm(193THz),B=2nm(0.25THz), N = 1

and Depth = 100dB.

3.3.8 Dispersion Compensation Fiber

The optical fiber component simulates the propagation of an optical field in a single-mode fiber with the dispersive and nonlinear effects taken into account by a direct numerical integration of the modified nonlinear Schrödinger (NLS) equation (when the scalar case is considered) and a system of two, coupled NLS equations when the polarization state of the signal is arbitrary. The optical sampled signals reside in a single frequency band, hence the name total field. The parameterized signals and noise bins are only attenuated.

3.3.9 Fiber Bragg Grating (FBG)

The non-uniform (chirped and apodized) grating is divided into Number of Segments uniform gratings. The coupled mode theory is used to calculate the scattering matrix of each uniform segment, and the spectral response of the whole grating is found by connecting the uniform segments using the transfer matrix theory. The apodization functions Gaussian and Hyperbolic tangent are defined with the following parameters:

Gaussian

$$A(z) = \exp\{-ln2.[\frac{2(z-L/2)}{S.L}]^2\} \quad (3.9)$$

Hyperbolic tangent

$$A(z) = \tanh(s.z/L).\tanh[s.(1-z/L)] + 1 - \tanh^2(s/2). \quad (3.10)$$

3.3.10 Optical Infinite Impulse Response Filter

The optical infinite impulse response filter is a recursive digital filter. The transfer function can be expressed in the z domain as.

$$H(z) = \frac{\alpha \sum_{n=0}^{N} a_n z^{-n}}{\sum_{m=0}^{M} b_m z^{-m}} \quad (3.11)$$

Where H(z) is the filter transfer function in the Z domain, α is the parameter for Additional loss, N is the parameter number of Numerator coefficients, α_n are the coefficients for the numerator, M is the parameter number of Denominator coefficients, and b_m are the coefficients for the denominator.

Also,

$$Z = \exp\left(\frac{j2\pi(f-f_c)}{f_s}\right) \quad (3.12)$$

Where f_c is the filter center frequency defined by the parameter frequency, f_S is the parameter Filter sample rate, and f is the frequency. Where f = 1552.5nm(193THz), f_s = 500GH_z, a_n = 2,

N = 0.0355083, b_m = 2 and M = 0.96449.

According to the parameter Filter coefficients type, the filter transfer function can be given in the z(z domain) or in the frequency domain. In the second case, the filter is determined by the numerator and the denominator polynomial, which can be expressed by their roots (poles and zeros) or by the polynomial coefficients (in frequency domain).

Note: Individual samples require that the filter coefficients are given in the z domain.

3.4 Minimization Of Four Wave Mixing Parameters

In this study, the parameters of the minimization of four wave mixing are studied. The parameters referred to includes the input and output parameters. The input parameters referred to as the design parameters that can be adjusted, so that the best performance of the minimization of FWM system can be obtained. The input parameters considered in this simulation research includes Input power (CW laser power), CW laser wavelength, frequency, effective area, channel spacing, dispersion, and fiber length (length of optical fiber). The output parameters can be defined as the performance measure parameters obtained as a result of variation in design parameters. The performance parameters considered in this study includes signal power, noise power, OSNR, FWM sideband, and threshold value of input power.

3.4.1 Design Parameters

The design parameters referred to as input parameters of the four wave mixing that alter for the purpose of the FWM minimization. The deign parameters considered in this study includes Input power (CW laser power), CW laser wavelength, frequency, effective area, channel spacing, dispersion, and fiber length (length of optical fiber).

The details about these parameters are discussed as follows.

3.4.1.1 Input Power (CW laser power)

The power of a laser is measured in watts and often reported in terms of nW, mW, W etc. This is referring to the optical power output of the laser beam, which is the continuous power output of continuous wave (CW) lasers, or the average power of a pulsed or modulated laser.

In this research the input power level was varied for 41dBm to – 10 dBm because at 40dBm the threshold value of input power for Optical IIR filter was obtained, below which the OSNR is constant.

3.4.1.2 Frequency

The optical frequency, for example of a quasi – monochromatic laser beam is the oscillation frequency of the corresponding electromagnetic wave. For visible light, optical frequencies are roughly between 400THz (terahertz = 10^{12}Hz) and 700THz, corresponding to vacuum wavelengths between 700nm and 400nm. In this research frequency value of 2.4GHz was utilized because it falls within the microwave range of frequencies.

3.4.1.3 Channel Spacing

The amount of bandwidth allotted to each channel in a communication system that transmits multiple frequencies such as fiber optics. It is measured as the spacing between center frequencies (or wavelengths) of adjacent channels.

In this research channel spacing of 1nm was used so as to differentiate the allocated frequencies and also because an increase in channel spacing from 1550nm to 1551nm reduces the FWM effect and for the unequal channel spacing wavelengths of 1550nm, 1550.3nm, 1550.2nm and 1550.4nm were used.

3.4.1.4 Effective Cross-sectional Area

The effect of nonlinearity grows with intensity in fiber and the intensity is inversely proportional to area of the core. Since the power is not uniformly distributed within the cross-section of the fiber, it is reasonable to use effective cross-sectional area (A_{eff}). The A_{eff} is related to the actual area (A)and the cross-sectional distribution of intensity $I(r, \theta)$ in following way,

$$A_{eff} = \left[\frac{\int_r \int_\theta r dr d\theta I(r,\theta)}{\int_r \int_\theta r dr d\theta I^2(r,\theta)} \right] \tag{3.13}$$

Where r and ɵ denote the polar coordinates. Figure 3.5 provides definition of effective area (A_{eff}).

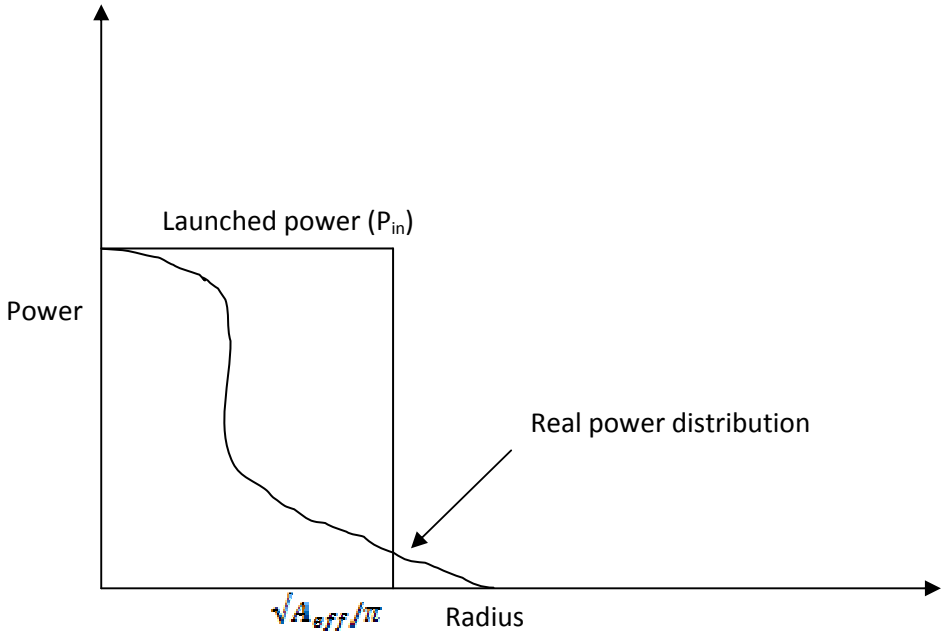

Fig. 3.5: Definition of Effective Core Area. (Maxim Integrated, 2016).

3.4.1.5 Effective Transmission Length

The nonlinear effects depend on transmission length. The longer the fiber link length, the more the light interaction and greater the nonlinear effect. As the optical beam propagates along the link length, its power decreases because of fiber attenuation. The effective length (L_{eff}) is that length, up to which power is assumed to be constant. The optical power at a distance z along link is given as,

$$P(z) = P_{in} \exp(-\alpha z) \tag{3.14}$$

Where $P_{in}$is the input power (power at z = 0) and α is coefficient of attenuation. For actual link length *(L)*, effective length is defined as.

$$P_{in} L_{eff} = \int_{z=0}^{L} P(z) dz \tag{3.15}$$

Using the two equations above, effective link length is obtained as,

$$L_{eff} = \frac{(1-\exp(-\alpha z))}{\alpha} \tag{3.16}$$

Since communication fibers are long enough so that $L \gg 1/\alpha$. This results in $L_{eff} \approx 1/\alpha$.

3.4.2 Performance Parameter

The performance parameters as discussed earlier are the output parameters used to measure the performance of the minimization of four wave mixing effect. In this thesis various performance parameters were considered to evaluate and represent the working conditions of the minimization of FWM effect. The performance parameter are: signal power, noise power, optical signal to noise ratio (OSNR),four wave mixing sideband, and threshold value of input power.

3.4.2.1 Signal Power

The power in an optical signal can be defined as the magnitude of the vector cross product of an electric and magnetic fields, which can be written and simplified as follows:

$$P_o(t) = /\vec{E}(t) \times \vec{H}(t)/ = /\vec{E}(t)/ = \frac{/\vec{E}(t)/}{\eta} = \frac{/\vec{E}(t)/^2}{\eta} \tag{3.17}$$

Where the notation 1x1 represents the magnitude of X, and n = $\sqrt{\frac{\mu}{\varepsilon}}$is the optical impedance of the fiber (μ = permeability and ε = permittivity)

Recognizing that there are only two discrete power levels leads to the optical equivalent , i.e.,

$$S_{OL} = \frac{/\vec{E}_L/^2}{\eta} \text{ and } S_{OH} = \frac{/\vec{E}_H/^2}{\eta} \quad (3.18)$$

Where S_O represents optical signal power and the subscripts L and H represent the low and high power or low and high electric field strengths associated with a binary zero or one respectively.

3.4.2.2 Noise Power

Noise can be defined as any unwanted or interfering signal other than the one that is intended or expected. In general, the noises associated with the high and low signal levels in binary optical digital communications each have a different value. The mean – square average electrical and optical noise powers can be computed mathematically using the following equations.

$$N_E = \frac{1}{T}\int_0^T i_N^2(t)Rdt = \sigma_1^2 R \quad (3.19)$$

$$= \frac{1}{T}\int_0^T v_N^2(t)\frac{1}{R}dt = \sigma_v^2\frac{1}{R} \quad (3.20)$$

$$N_o = \frac{1}{T}\int_0^T /\overrightarrow{E_N}(t)/^2\frac{1}{n}dt = \sigma_0^2\frac{1}{n} \quad (3.21)$$

Where N is the noise power, T is the integration period, σ^2 is the mean-square average power, and the subscript N signifies that the associated current, voltage or electric field is classified as noise.

3.4.2.3 Optical Signal-to-Noise Ratio (OSNR)

Knowledge of the ratio of the signal power to the noise power (signal-to-noise ratio or SNR) is important because it is directly related to the bit error ratio (BER) in digital communication systems, and the BER is a major indicator of the quality of the overall system.

We can mathematically express the electrical SNR as

$$SNR_E = \frac{S_E}{N_E} = \frac{v^2/R}{\sigma_v^2/R} = \frac{v^2}{\sigma_v^2} \tag{3.22}$$

$$= \frac{i^2 R}{\sigma_i^2 R} = \frac{i^2}{\sigma_i^2} \tag{3.23}$$

Similarly, the optical SNR is

$$SNR_0 = \frac{S_0}{N_0} = \frac{|E|^2 \frac{\eta}{2}}{\sigma_0^2 \frac{\eta}{2}} = \frac{|E|^2}{\sigma_0^2} \tag{3.24}$$

In practice, optical powers are rarely measured directly. Instead, the optical power is converted to a proportional electric current using a device such as a PIN photodiode, and then the current is measured. The ratio between the output current and the incident optical power is called the responsively (mathematically represented using the symbol R) which has the units of Amperes per Watt (A/W). It is important to note that the conversion between optical power (units of Watts) and electrical current (units of Amperes) essentially results in a square root operation. Electrical power is related to the square of the voltage or current. Optical power is related to the square of the magnitude of the electric field. The result is that the conversion between optical signal or noise power, (S_o or N_o – both related to $|E|^2$) and electrical current results in what is essentially a square root relationship, i.e.

$$i_{signal} = S_o R \text{and} i_{noise} = N_o R \tag{3.25}$$

Also, the optical SNR, when converted to an electrical SNR, is equal to the square root of the equivalent electrical SNR. This is illustrated mathematically by combining equations above as follows:

$$\sqrt{SNR_E} = \sqrt{\frac{S_E}{N_E}} = \frac{i_{signal}}{\sigma_i} = \frac{S_o R}{N_o R} = SNR_o \tag{3.26}$$

3.5 Conclusion

The design of minimization of four wave mixing (MFWM) are based on simulation carried out in simulation environment of optisystem optical simulation software. The principle of operation of MFWM was properly discussed. Brief explanations on the MFWM parameters and components have been given in order to have a better understanding of the construction of the MFWM effects.

CHAPTER FOUR

RESULTS AND DISCUSSIONS

4.1 Introduction

This chapter presents the results of the simulation of minimization of FWM effect through optisystem optical simulation software. The results of the effect of input parameters such as input power(CW laser power), CW laser wavelength, frequency, effective area, channel spacing, dispersion, fiber length(length of optical fiber) on performance parameters are properly analyzed where necessary. The performance parameters considered in this study includes signal power, noise power, optical signal to noise ratio (OSNR), four wave mixing sideband, and the threshold value of input power. The measuring tools used in this simulation includes optical spectrum analyzer, WDM analyzer and optical power meter.

4.2 Effect of Polarization Controller on Four Wave Mixing Effect.

The spectrums in Figures 4.1, 4.2, 4.3, and 4.4 shows the four wave mixing sidebands. The channel spacing was set at 1nm (1550nm to 1551nm) so as to differentiate the allocated frequencies and also because an increase in channel spacing from 1550nm to 1551nm reduces the FWM effect, with input powers of 0dBm, -4dBm, -8dBm and -10dBm respectively. The performance at0dBm shows maximum FWM sideband of -80dBm.This shows improvement over (Jain and Therese) because at 0dBm the maximum FWM sideband obtained was -69.6dBmwhich is higher as compared to -80dBm FWM sideband realized in this work. The figure 4.5 shows clearly the result of the work of (Jain and Therese). The reason for this performance is because of the incorporation of polarization controller in this work unlike in (Jain and Therese). This is due to the fact that the polarization controller(PC) controls the state of polarization of light within the fiber core and then sets the input signal in an arbitrary

polarization state. The polarization controller adjusts the first two incident waves to linear polarization. The PC controls the polarization angle between the pump light and the signal light. With the polarization controller most of the FWM frequencies were cancelled because the interaction between multiple optical channels that pass through the same fiber reduced, which suppressed the FWM. The interfering wavelengths generated around the original two wavelength system are 1549nm and 1552nm. Further when we decreased the power level from 24dBm to -10dBm, the input power level was compared with the noise power and signal to noise ratio to find the threshold power level. Table 4.1 below shows the output of the WDM analyzer giving the value of the noise power and the OSNR with respect to the input signal power, as the input power level increases, the signal power also increases. Figure 4.6 below shows the graph of the input power and noise power, as the input power level decreases, the noise power also decreases. Figure 4.7 below shows the graph of the input power level and OSNR, the threshold value of input power is found to be 22dBm below which the OSNR is constant.

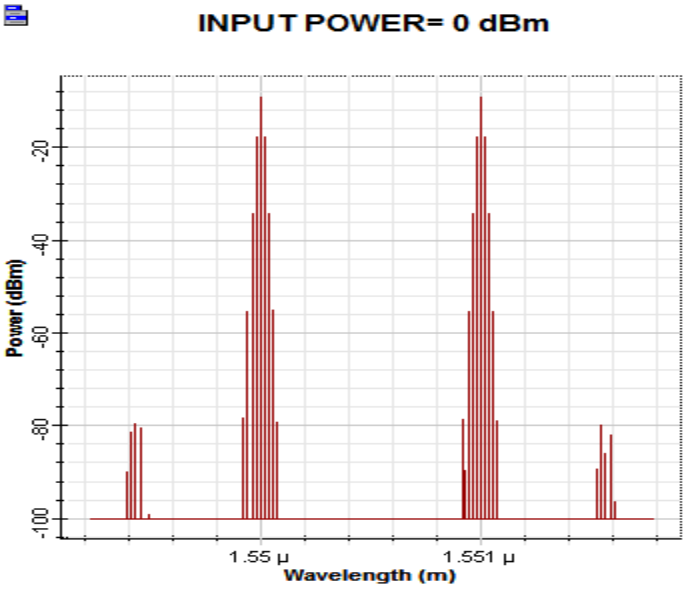

Figure 4.1: The optical spectrums at the output when the two wavelengths are transmitted at 0dBm.

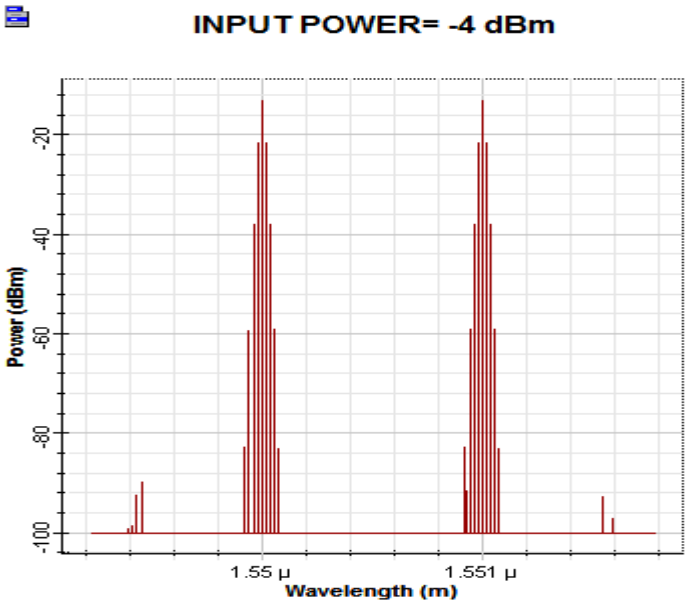

Figure 4.2: The optical spectrums at the output when the two wavelengths are transmitted at -4dBm.

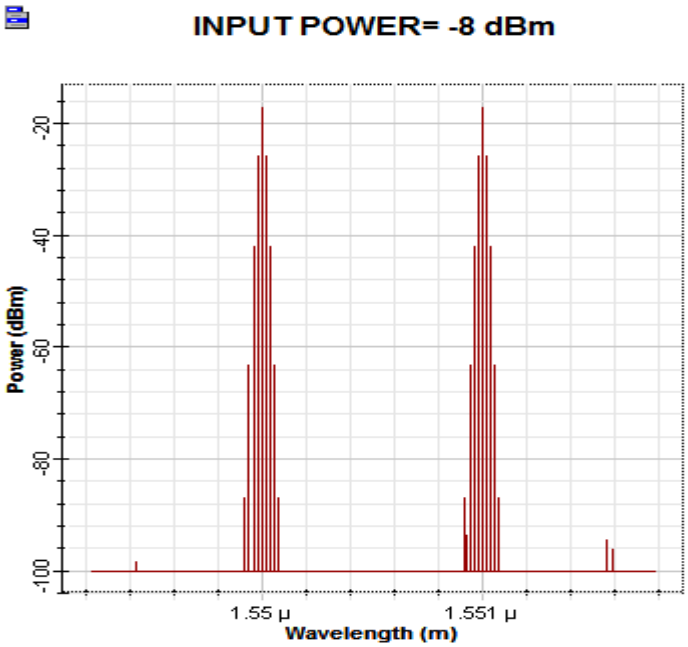

Figure 4.3: The optical spectrums at the output when the two wavelengths are transmitted at -8dBm.

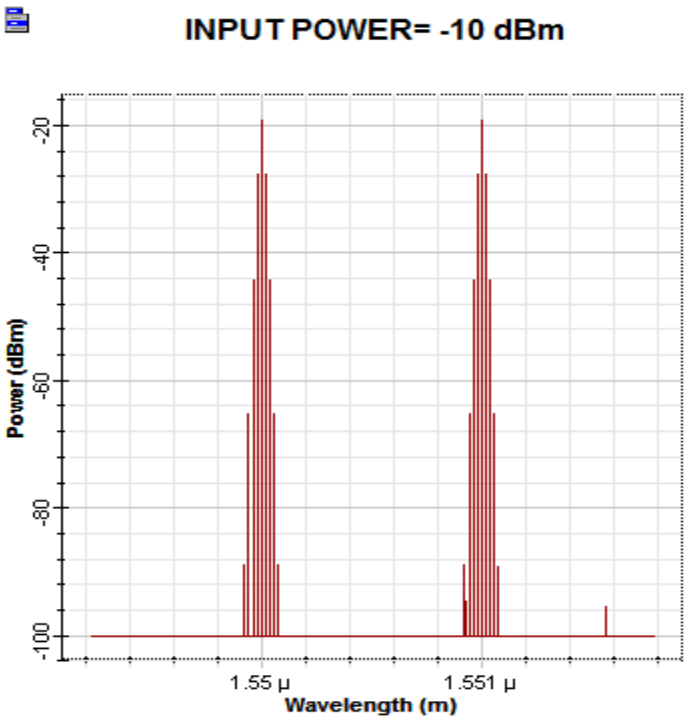

Figure 4.4: The optical spectrums at the output when the two wavelengths are transmitted at -10dBm

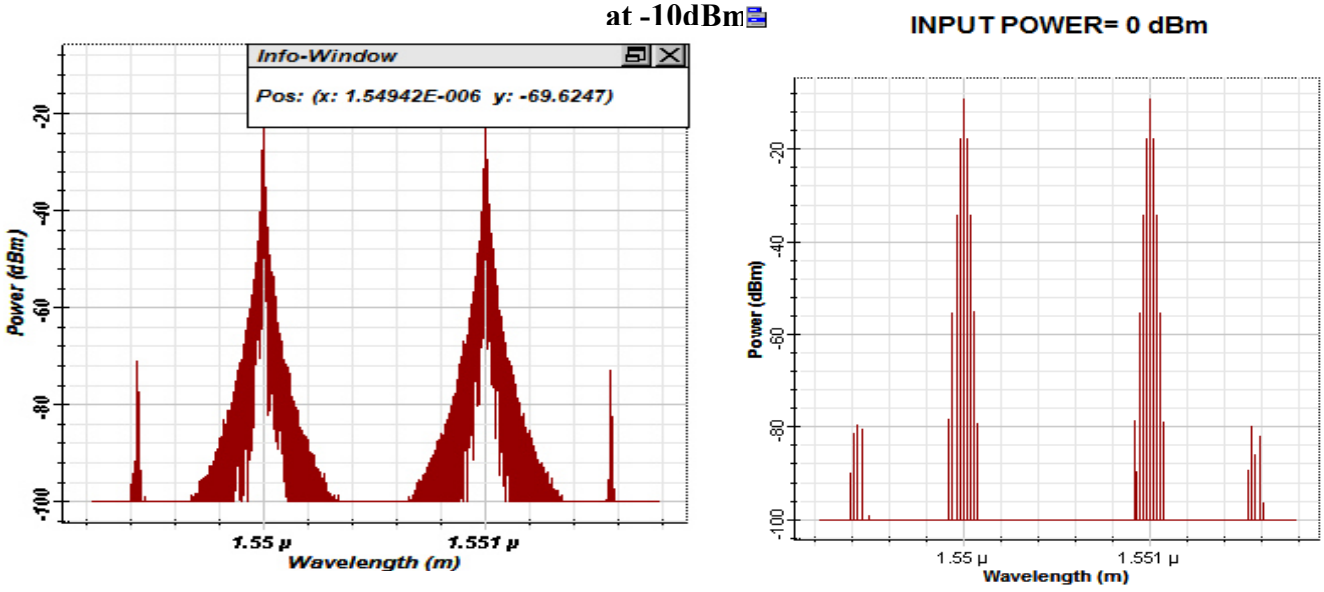

Figures 4.5: The optical spectrums at the output when the two wavelengths are transmitted at 0dBm. (a) (Jain and Therese). (b) Proposed work.

Table 4.1: Comparison of Parameters for Different Input Power

Input Power (In dBm)	Signal Power (In dBm)	Noise Power (In dBm)	OSNR (dB)
24	15.80	-43.30	59.10
22	13.80	-50.22	78.30
20	11.80	-56.89	78.30
10	1.80	-80.71	78.30
0	-8.20	-82.03	78.30
-4	-12.20	-92.37	78.29
-8	-16.20	-98.32	78.29
-10	-18.20	-100	78.29

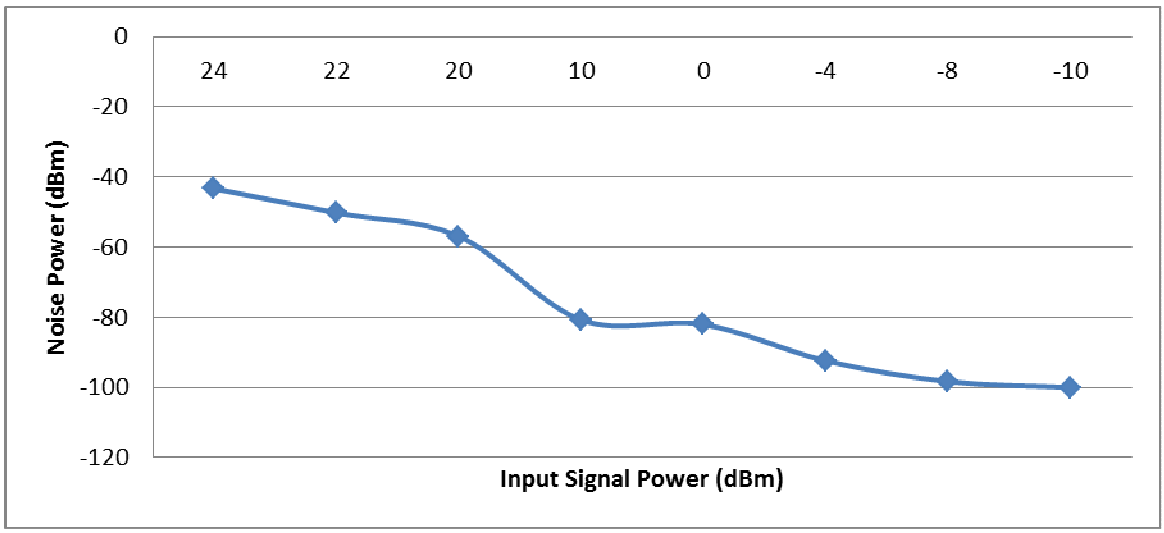

Fig. 4.6: Graph of Input Signal power and Noise Power

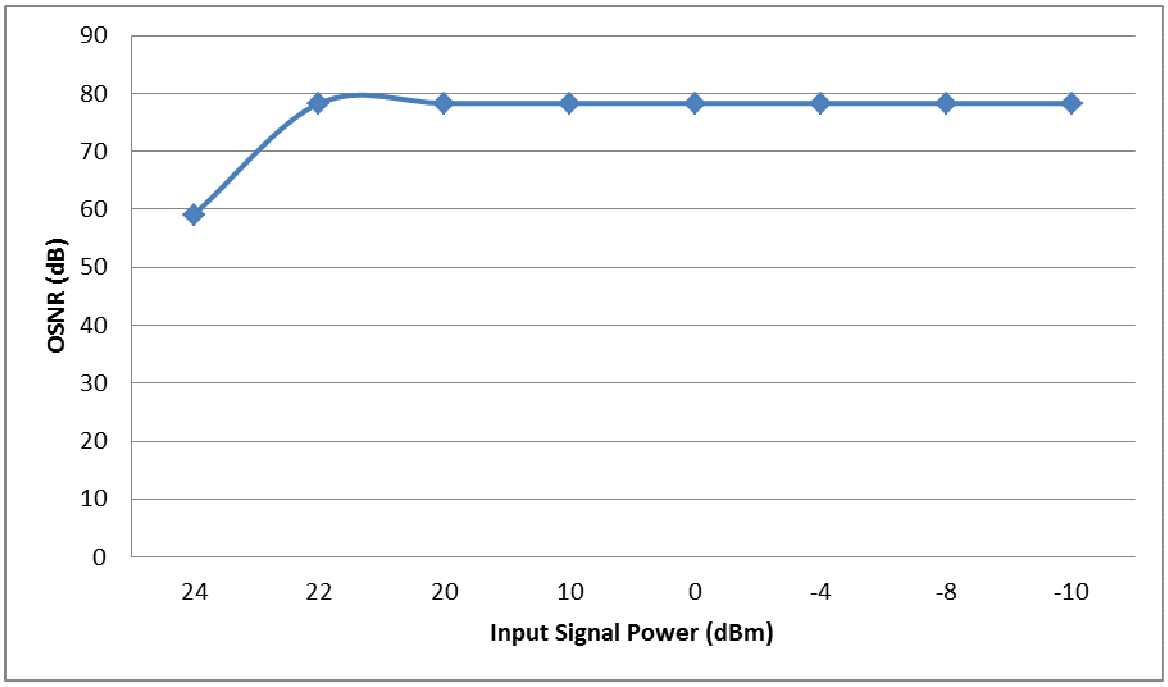

Fig.4.7: Graph of Input Signal Power and OSNR

Further decrease in power level from 24dBm to 10dBm, the sideband of FWM is increasing due to the pronounced effect of the signal degradation of FWM as a result of low noise in the channel. This is clearly shown in Figure 4.6. The effect of the input power on OSNR, signal power and noise power is compared and comprehensively shown in Table 4.1,as the input power level increases, the signal power also increases. Figure 4.6, as the input power decreases, the noise power also decreases and Figure 4.7 where the threshold value of the input power is found to be 22dBm below which the optical signal to noise ratio (OSNR) is constant.

4.3 Effect of Bessel Optical Filter on Four Wave Mixing Effect

The spectrums in Figures 4.8, 4.9, 4.10 show the four wave mixing sidebands. The channel spacing was set at 1nm (1550nm to 1551nm) so as to differentiate the allocated frequencies and also because an increase in channel spacing from 1550nm to 1551nm reduces the FWM effect, with input powers of 0dBm, -4dBm and -8dBm respectively. The performance

at 0dBm shows maximum FWM sideband of -84dBm. This shows improvement over (Jain and Therese) because at 0dBm the maximum FWM sideband obtained was -69.6dBm which is higher as compared to -84dBm FWM sideband realized in this work. The figure 4.11 shows clearly the result of the work of (Jain and Therese). The reason for this performance is because of the incorporation of bessel optical filter (BOF) in this work unlike in (Jain and Therese). This is due to the fact that the bessel optical filter is an optical filter with a Bessel frequency transfer function and also due to the self-healing property of the bessel beam, the extended depth and tight focusing features of the bessel beam. Also the bessel optical filter can automatically distinguish between the active wavelength and the newly generated wavelength by the algorithm programmed inside the filter which leads to a dramatic reduction in FWM. Also BOF drops multiple undesired frequencies that appear with the optical channels and BOF damp all FWM wavelengths in parallel that may appear with the main signals in the WDM system. When we decreased the power level from 29dBm to -10dBm, the input power level was compared with the noise power and the optical signal to noise ratio (OSNR) to find the threshold power level. Table 4.2 shows the output of the WDM analyzer giving the value of the noise power and optical signal to noise ratio (OSNR) with respect to the input signal power, as the input power level increases, the signal power also increases. Figure 4.12 shows the graph of the input power level with the noise power, as the input power level decreases, the noise power also decreases. Figure 4.13 shows the graph of the input power level and optical signal to noise ratio (OSNR), the threshold value of input power is found to be 27dBm below which the OSNR is constant.

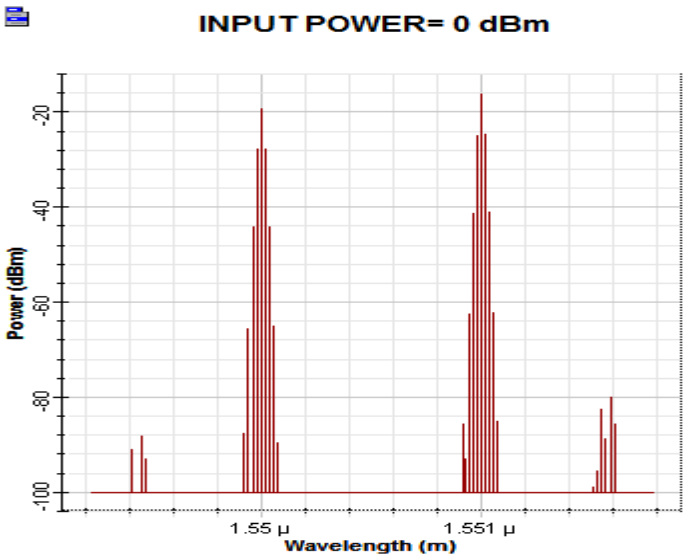

Figure 4.8: The optical spectrums at the output when the two wavelengths are transmitted at 0dBm.

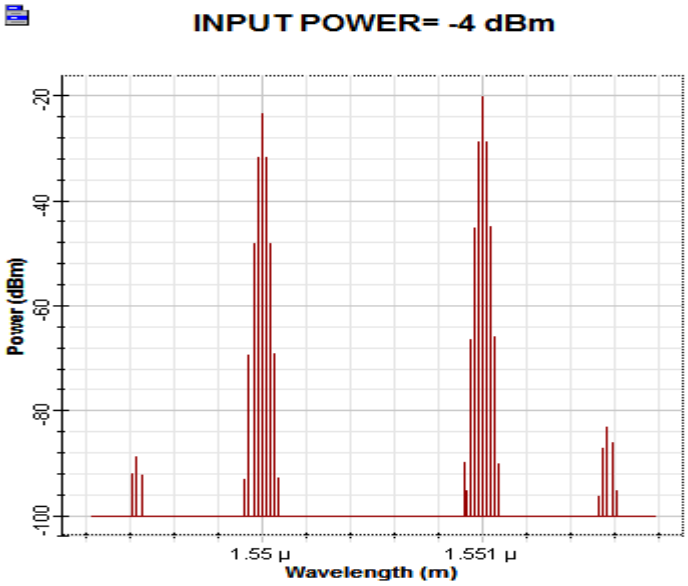

Figure 4.9: The optical spectrums at the output when the two wavelengths are transmitted at -4dBm.

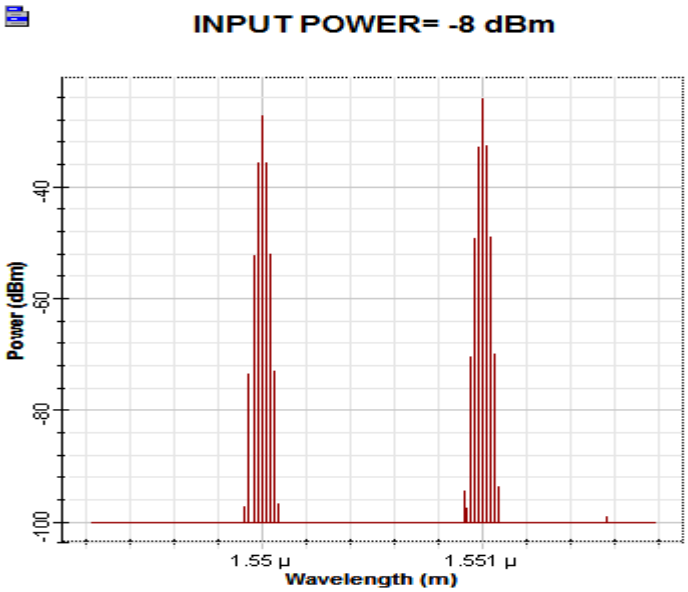

Fig. 4.10: The optical spectrums at the output when the two wavelengths are transmitted at -8dBm.

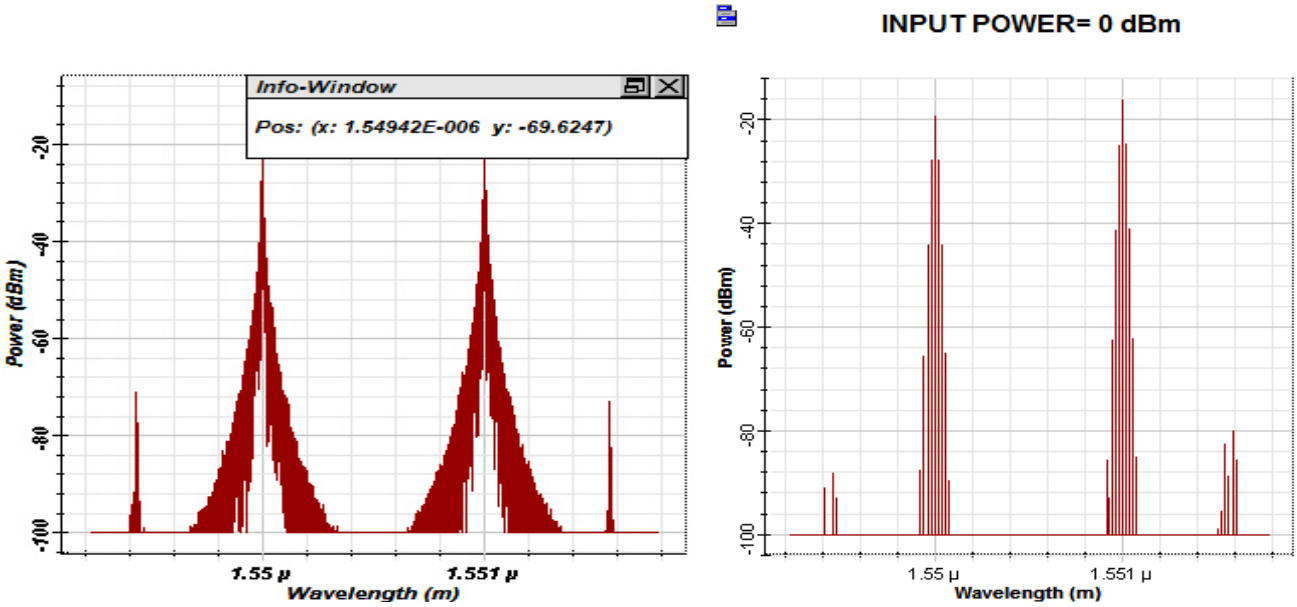

Figure 4.11: The optical spectrums at the output when the two wavelengths are transmitted at 0dBm (a) (Jain and Therese). (b) Proposed work.

Table 4.2: Comparison of Parameters for Different Input Power

Input power (in dBm)	Signal power (in dBm)	Noise power (in dBm)	OSNR (dB)
29	13.56	-30.77	44.33
27	11.74	-37.59	68.20
25	9.78	-44.69	68.20
20	4.80	-61.32	68.20
10	-5.20	-78.09	68.20
0	-15.20	-93.55	68.20
-4	-19.20	-100	68.20
-8	-23.20	-100	68.17
-10	-25.20	-100	68.17

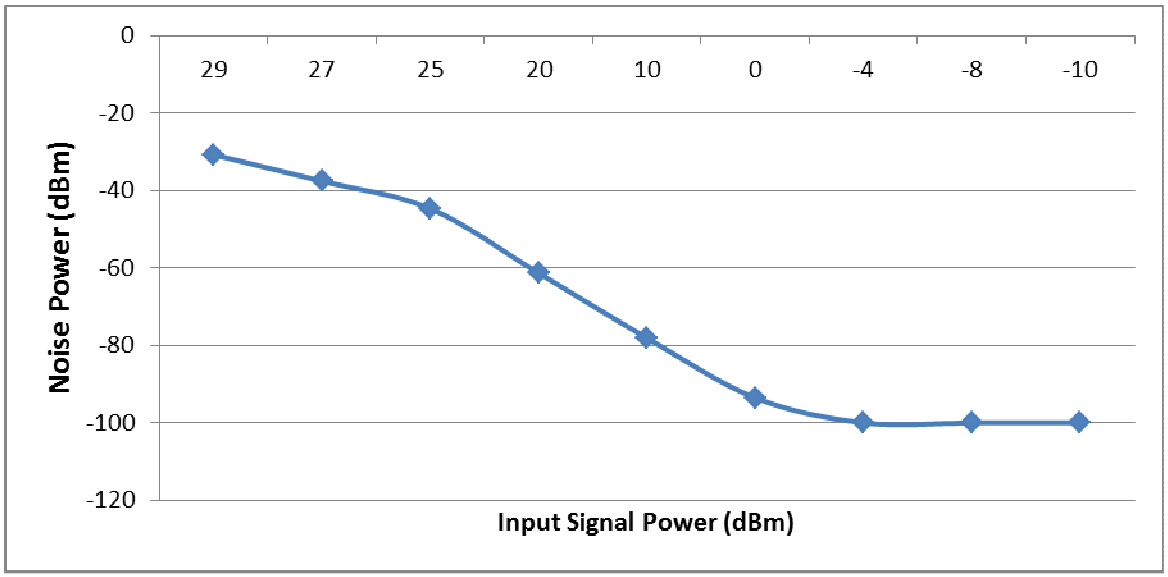

Fig.4.12: Graph of Input Signal Power and Noise Power

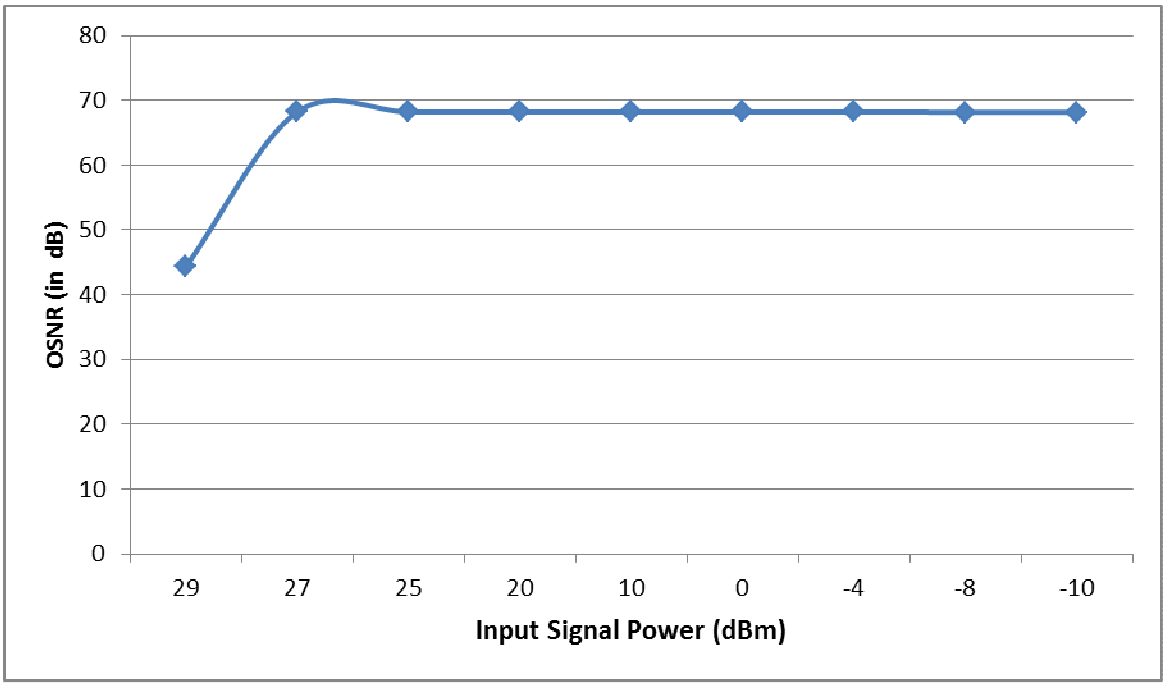

Fig. 4.13: Graph of Input Signal Power and OSNR

Further decrease in power level from 29dBm to 10dBm, the sideband of FWM is increasing due to the pronounced effect of the signal degradation of FWM as a result of low noise in the channel. This is clearly shown in Figure 4.12. The effect of the input power on OSNR, signal power and noise power is compared and comprehensively shown in Table 4.2, as the input power level increases, the signal power also increases. Figure 4.12, as the input power level decreases, the noise power also decreases and Figure 4.13 where the threshold value of input power is found to be 27dBm below which the optical signal to noise ratio (OSNR) is constant.

4.4 Effect of Dispersion Compensation Fiber and Fiber Bragg Grating on Four Wave Mixing Effect.

The spectrums in Figures 4.14, 4.15 and 4.16 show the four wave mixing sidebands. The channel spacing was set at 1nm with input powers of 0dBm, -4dBm and -8dBm respectively.

The performance at 0dBm shows maximum FWM sideband of -85dBm. This shows improvement over (Jain and Therese) because at 0dBm the maximum FWM sideband obtained was -69.6dBm which is higher as compared to -85dBm FWM sideband realized in this work. The figure 4.17 shows clearly the result of the work of (Jain and Therese). The reason for this performance is because of the incorporation of dispersion compensation fiber and fiber bragg grating in this work unlike in (Jain and Therese). This is due to the fact that in the dispersion compensation fiber the optical fiber component simulates the propagation of an optical field in a single mode fiber with the dispersive and nonlinear effects taken into account by a direct numerical integration of the modified nonlinear Schrodinger (NLS) equation and in the fiber bragg grating, the non-uniform grating is divided into number of segments uniform gratings. Also the apodized FBGs given better system performance than the conventional FBGs and FBGs have low insertion loss. The apodized grating play a very important role to suppress FWM sideband and maintaining the reflectivity and narrow bandwidth. According to fiber specification the chirp characteristics is readily chosen. To tolerate high optical power without any loss due to non-linear effect is prominent characteristics that separate the DCF and FBG from DCF. At low optical power the DCF show non-linearity effect, but at high power DCF and FBG would not introduce such effect in optical network. The interfering wavelengths generated around the original two wavelength system are 1549nm and 1552nm. When we decreased the power level from 31dBm to -10dBm, the input power level was compared with the noise power and the optical signal to noise ratio (OSNR) to find the threshold power level. Table 4.3 shows the output of the WDM analyzer giving the value of the noise power and OSNR with respect to the input signal power, as the input power level increases, the signal power also increases. Figure 4.18 shows the graph of the input power level with the noise power, as the input power level decreases, the noise power also decreases. Figure 4.19 shows the graph of the input power

level and OSNR, the threshold value of input power is found to e 30dBm below which the OSNR is constant.

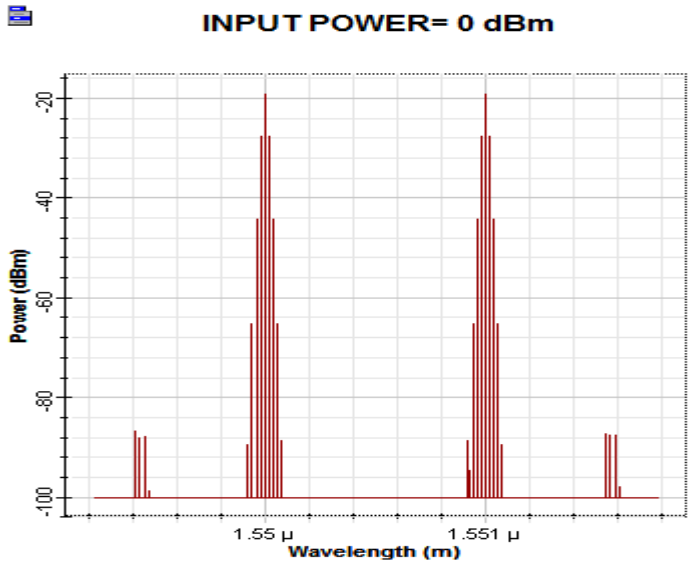

Figure 4.14: The optical spectrums at the output when the two wavelengths are transmitted at 0dBm.

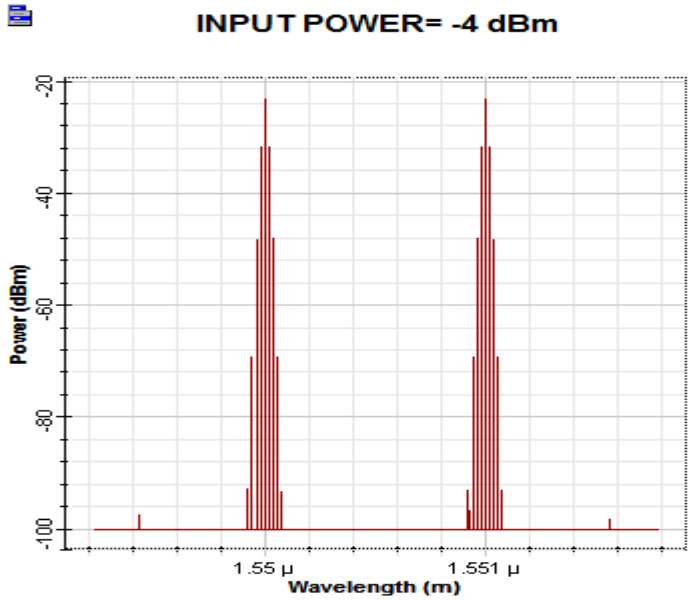

Figure 4.15: The optical spectrums at the output when the two wavelengths are transmitted at -4dBm.

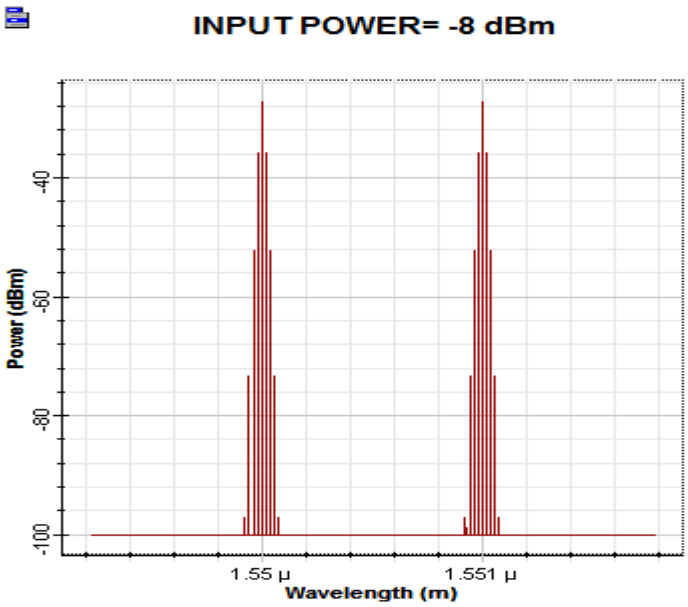

Figure 4.16: The optical spectrums at the output when the two wavelengths are transmitted at -8dBm.

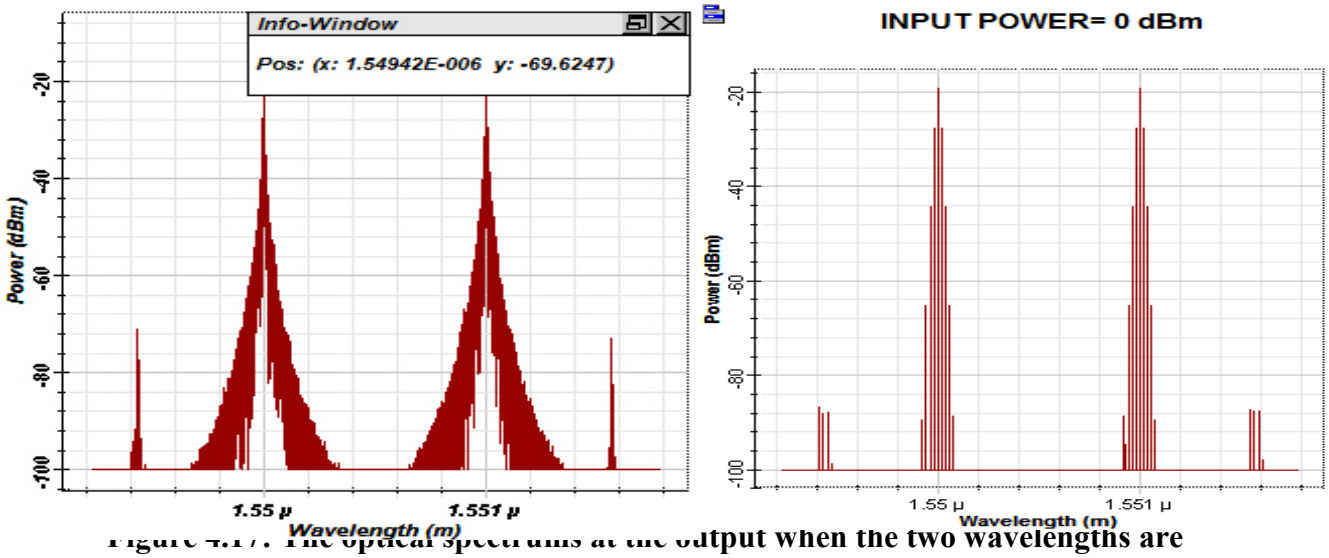

Figure 4.17: The optical spectrums at the output when the two wavelengths are transmitted at 0dBm (a) (Jain and Therese). (b) Proposed work.

Table 4.3: Comparison of Parameters for Different Input Power

Input Power (in dBm)	Signal Power (in dBm)	Noise Power (in dBm)	OSNR (in dB)
31	12.60	-24.45	37.01
30	11.70	-29.59	65.00
25	6.78	-45.12	65.00
20	1.79	-58.56	65.00
10	-8.21	-73.40	65.00
0	-18.21	-94.00	65.00
-4	-22.21	-100	64.73
-8	-26.21	-100	64.73
-10	-28.21	-100	64.73

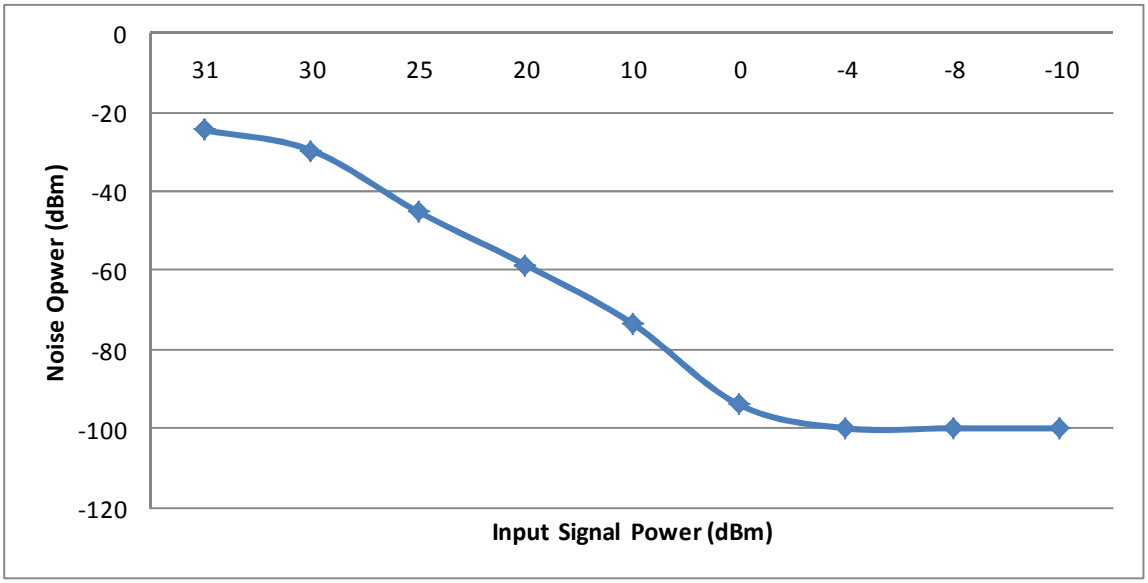

Fig. 4.18: Graph of Input Signal Power and Noise Power

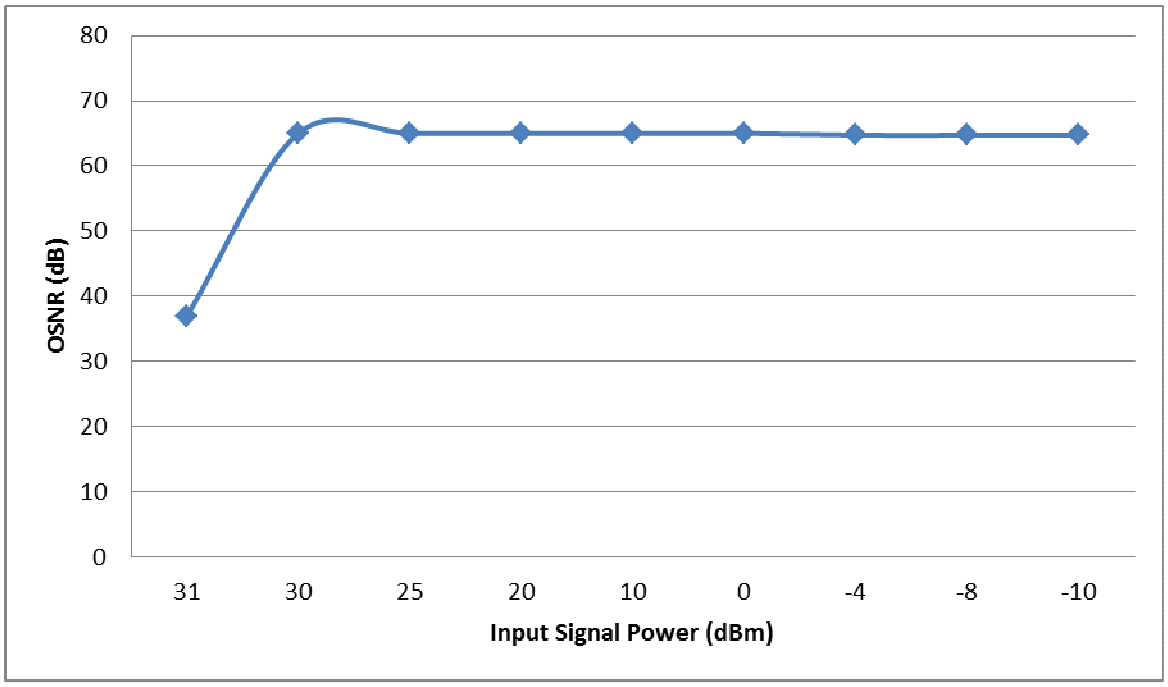

Fig.4.19: Graph of Input Signal Power and OSNR

Further decrease in power level from 31dBm to 10dBm, the sideband of FWM is increasing due to the pronounced effect of the signal degradation of FWM as a result of low noise in the channel. This is clearly shown in Figure 4.18. The effect of the input power on OSNR, signal power and noise power is compared and comprehensively shown in Table 4.3, as the input power level increases, the signal power level also increases. Figure 4.18, as the input power level decreases, the noise power also decreases and Figure 4.19 where the threshold value of input power is found to be 30dBm below which the optical signal to noise ratio (OSNR) is constant.

4.5 Effect of Unequal Channel Spacing on Four Wave Mixing Effect

The spectrums in Figures 4.20, 4.21 and 4.22 show the four wave mixing sidebands. The channel spacing was set at an unequal channel spacing of 1550nm, 1550.3nm, 1550.2nm and 1550.4nm with input powers of 0dBm, -4dBm and -8dBm respectively. The performance at 0dBm shows maximum FWM sideband of -88dBm. The reason for this performance is because

of the use of unequal channel spacing in this work. This is due to the fact that in the unequal channel spacing the unequal-spaced channel allocation design begins with the division of the available optical bandwidth into equal frequency slots of width and also since the difference between any two numbers is distinct, the new FWM frequencies generated would not fall into the one already assigned for the carrier channels. When we decreased the power level from 31dBm to -10dBm, the input power level was compared with the noise power and signal to noise ratio to find the threshold power level. Table 4.4 shows the output of the WDM analyzer giving the value of the noise power and optical signal to noise ratio (OSNR) with respect to the input signal power, as the input power level increases, the signal power also increases. Figure 4.23 shows the graph of the input power level with the noise power, as the input power level decreases, the noise power also decreases. Figure 4.24 shows the graph of the input power level with the OSNR, the threshold value of input power is found to be 30dBm below which OSNR is constant.

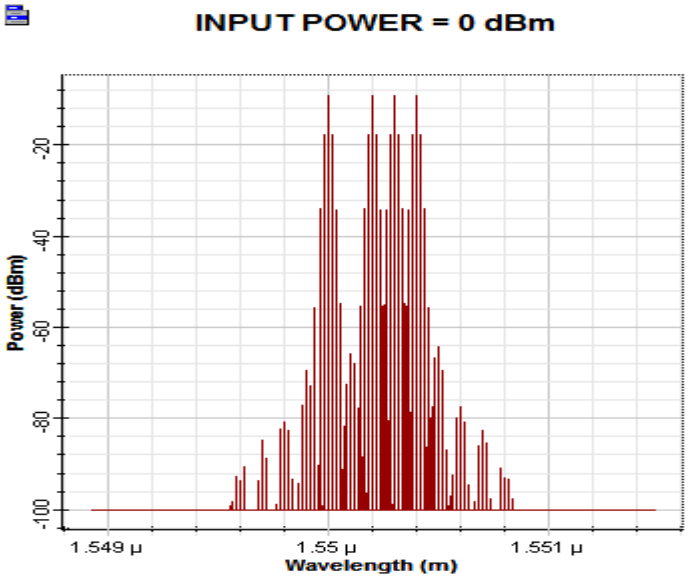

Figure 4.20: The optical spectrums at the output when the wavelengths are transmitted at 0dBm

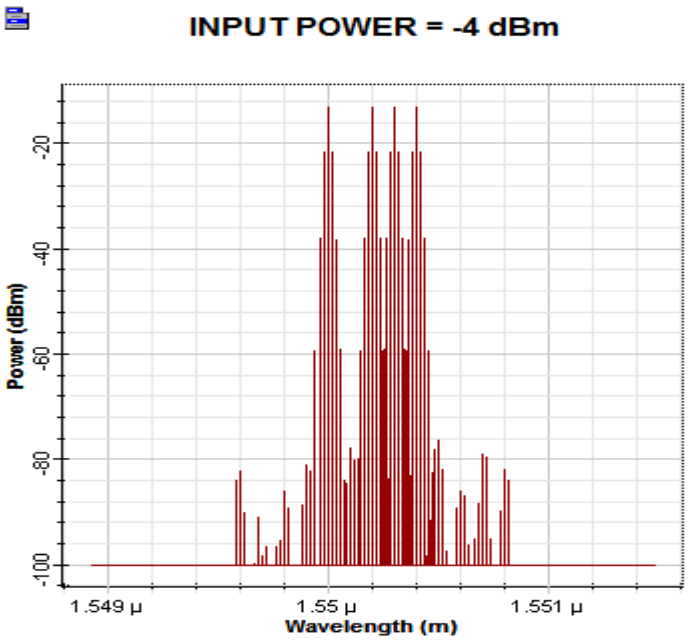

Figure 4.21: The optical spectrums at the output when the wavelengths are transmitted at -4dBm.

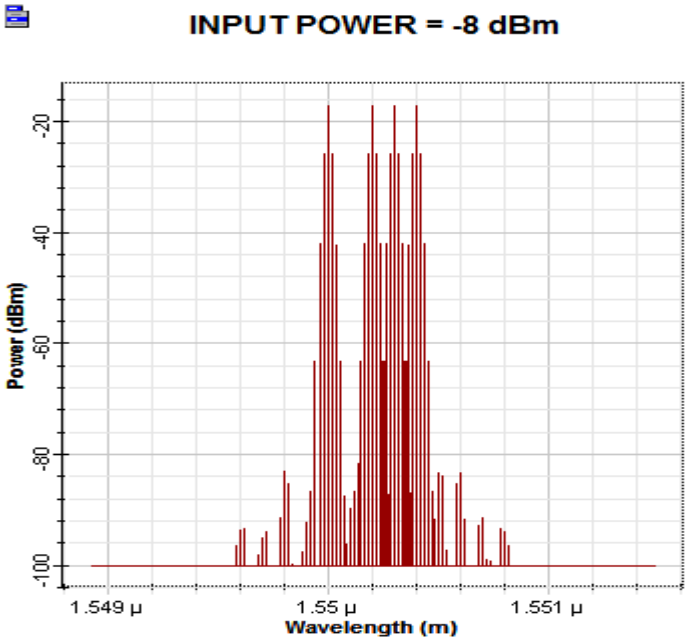

Figure 4.22: The optical spectrums at the output when the wavelengths are transmitted at -8dBm.

Table 4.4: Comparison of Parameters for Different Input Power

Input power (in dBm)	Signal power (in dBm)	Noise power (in dBm)	OSNR (dB)
31	20.66	13.85	6.82
30	19.84	12.58	51.11
25	16.61	-9.25	51.11
20	12.72	-23.58	51.11
10	1.81	-52.07	51.11
0	-8.20	-81.09	51.11
-4	-12.20	-80.26	51.11
-8	-16.20	-90.02	51.11
-10	-18.20	-90.59	51.11

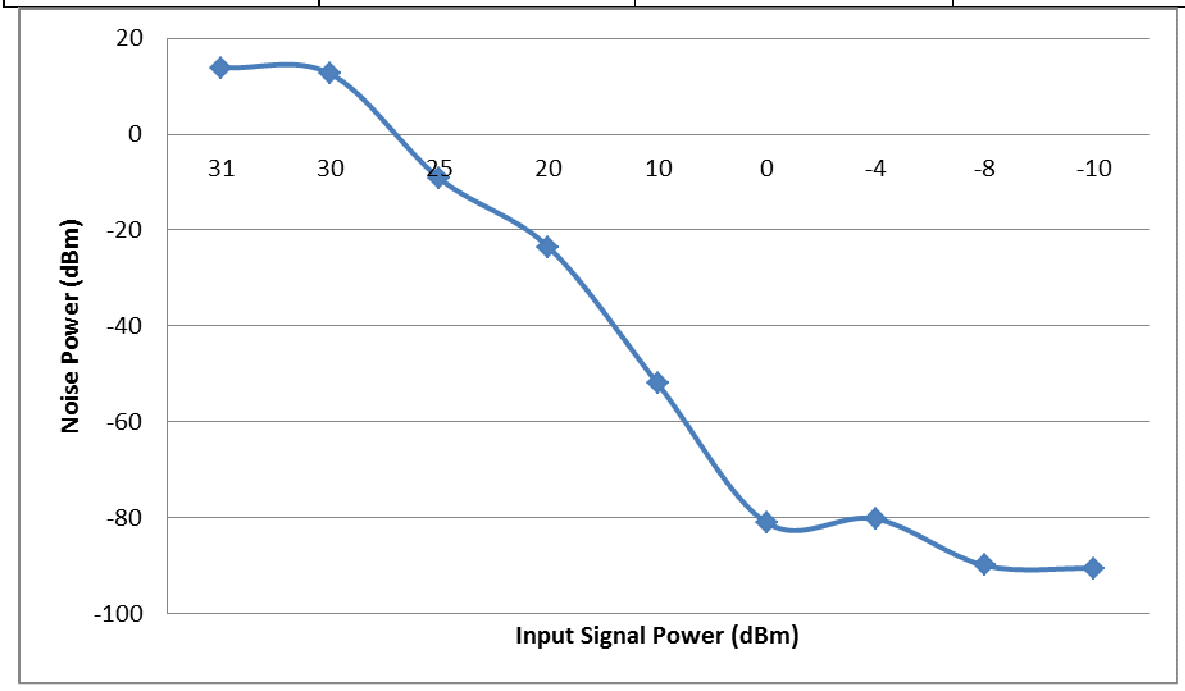

Fig.4.23: Graph of Input Signal Power and Noise Power

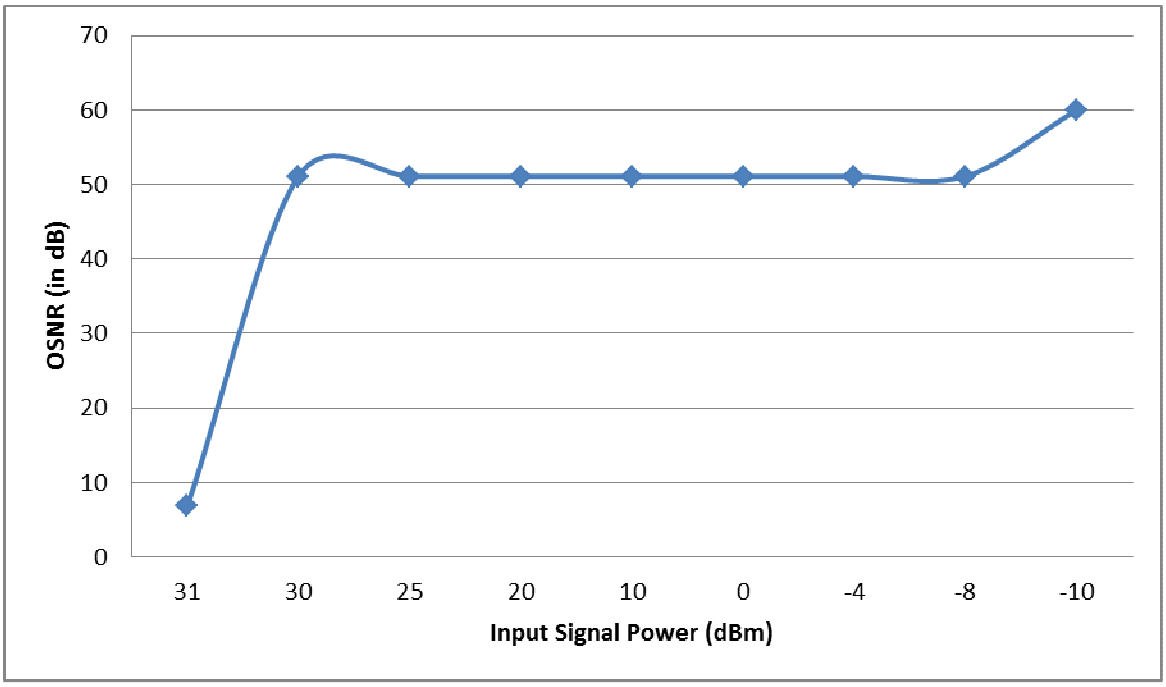

Fig.4.24: Graph of Input Signal Power and OSNR

Further decrease in power level from 31dBm to 10dBm, the sideband of FWM is increasing due to the pronounced effect of the signal degradation of FWM as a result of low noise in the channel. This is clearly shown in Figure 4.23. The effect of the input power on OSNR, signal power and noise power is compared and comprehensively shown in Table 4.4 where, as the input power level increases, the signal power also increases. Figure 4.23, as the input power level decreases, the noise power also decreases and Figure 4.24 where the threshold value of input power is found to be 30dBm below which the optical signal to noise ratio (OSNR) is constant.

4.6 Effect of Optical Infinite Impulse Response (Optical IIR) Filter on Four Wave Mixing Effect.

The spectrums in Figures 4.25, 4.26, and 4.27 shows the four wave mixing sidebands. The channel spacing was set at 1nm with input powers of 10dBm, 0dBm and -4dBm respectively.

The performance at 0dBm shows maximum FWM sideband of -99dBm. This shows improvement over (Jain and Therese) because at 0dBm the maximum FWM sideband obtained was -69.6dBm which is higher as compared to -99dBm FWM sideband realized in this work. The figure 4.28 shows clearly the result of the work of (Jain and Therese). The reason for this performance is because of the incorporation of optical infinite impulse response (optical IIR) filter in this work unlike in (Jain and Therese). This is due to the fact that the optical IIR filter is a recursive digital filter and also due to its efficiency and tolerance for loss. The optical IIR filter decomposes the desired filter response into a sum or difference of two all-pass filters. The filter responses are periodic, which is advantageous for WDM systems with more than one channel since the same filter can be used in different bands. The filter multichannel frequency selector has substantially better pass band flatness and stop band rejection than is possible with other filters having the same number of stages. The interfering wavelengths generated around the original two wavelength system are 1549nm and 1552nm. When we decreased the power level from 41dBm to -10dBm, the input power level was compared with the noise power and signal to noise ratio to find the threshold power level. Table 4.5 shows the output of the WDM analyzer giving the value of the noise power and optical signal to noise ratio (OSNR) with respect to the input signal power, as the input power level increases, the signal power also increases. Figure 4.29 shows the graph of the input power level with the noise power, as the input power level decreases, the noise power also decreases Figure 4.30 shows the graph of the input power level with the OSNR, the threshold value of input power is found to be 40dBm below which the OSNR is constant.

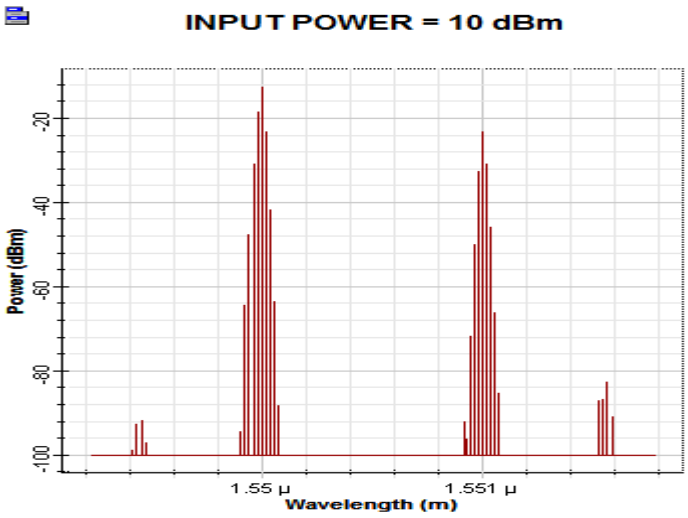

Figure 4.25: The optical spectrums at the output when the two wavelengths are transmitted at 10dBm.

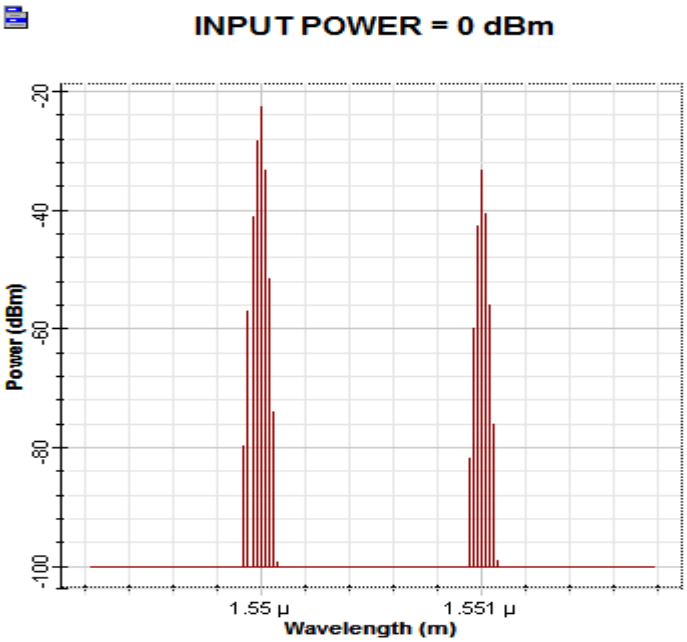

Figure 4.26: The optical spectrums at the output when the two wavelengths are transmitted at 0dBm.

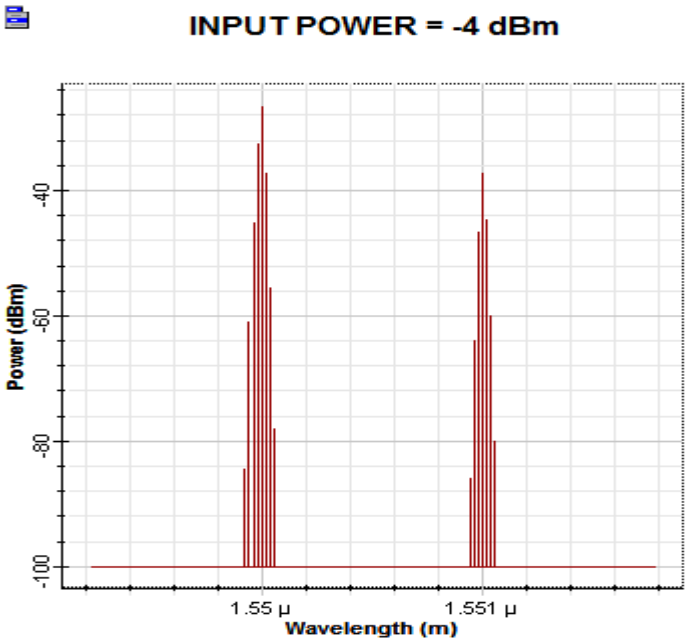

Figure 4.27: The optical spectrums at the output when the two wavelengths are transmitted at -4dBm.

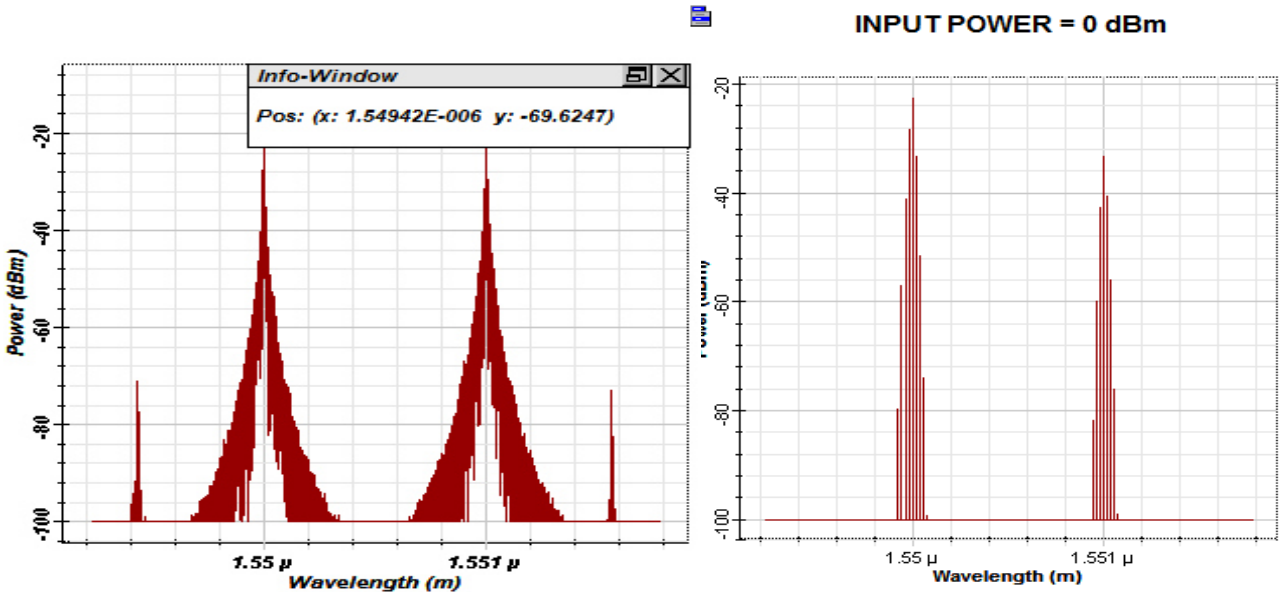

Figures 4.28: The optical spectrums at the output when the two wavelengths are transmitted at 0dBm (a) (Jain and Therese). (b) Proposed work

Table 4.5: Comparison of Parameters for Different Input Power

Input power (dBm)	Signal Power (dBm)	Noise Power (dBm)	OSNR (dB)
41	12.28	-14.02	26.30
40	11.16	-14.52	70.00
35	7.79	-27.03	70.00
30	8.81	-51.10	70.00
25	3.64	-68.96	70.00
20	-1.42	-85.88	70.00
10	-11.37	-100	70.00
0	-21.37	-100	70.00
-4	-25.37	-100	70.00
-8	-29.37	-100	70.00
-10	-31.37	-100	70.00

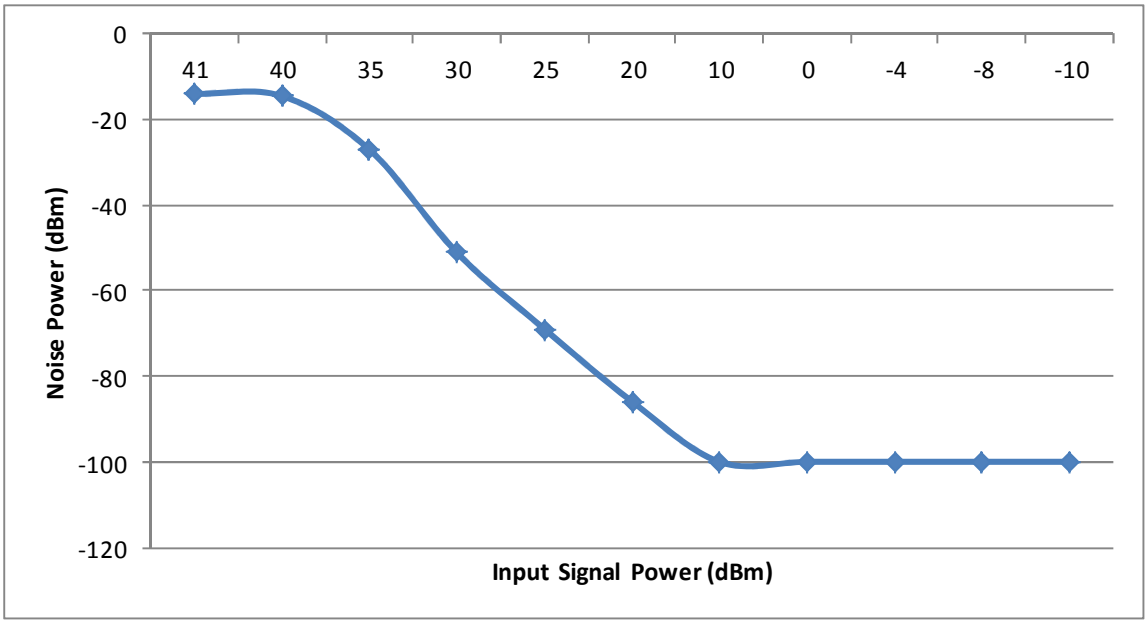

Fig. 4.29: Graph ofInput Signal Power and Noise Power

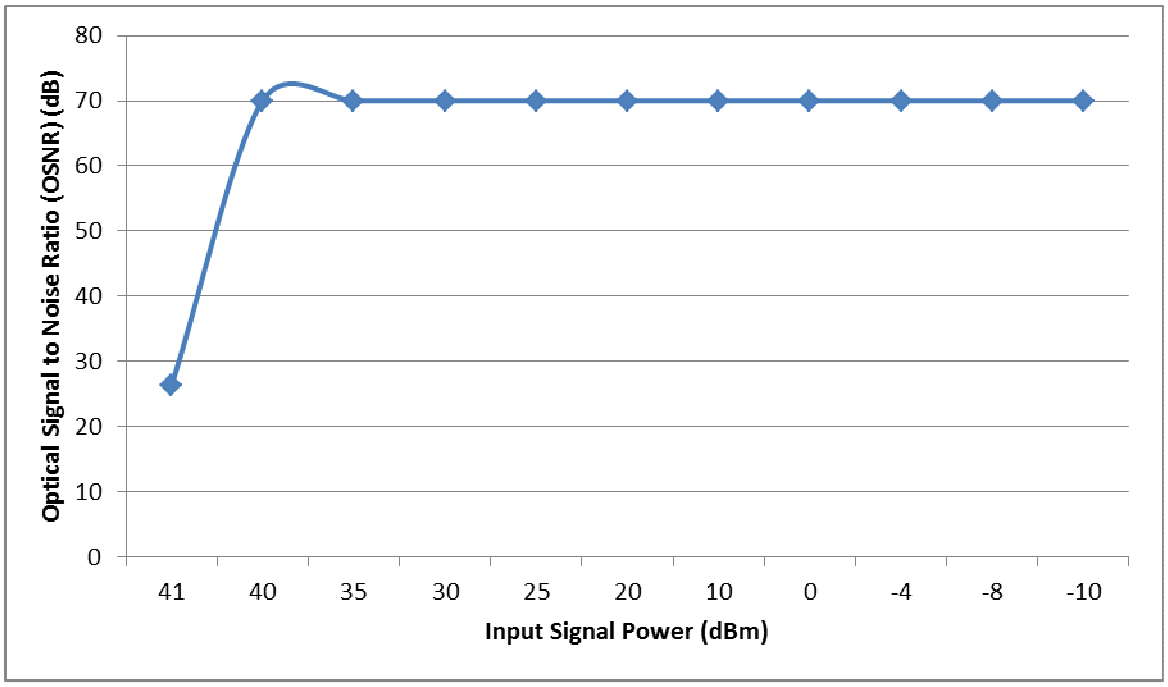

Fig.4.30:Graph of Input Signal Power and OSNR

Further decrease in power level from 41dBm to 20dBm, the sideband of FWM is increasing due to the pronounced effect of the signal degradation of FWM as a result of low noise in the channel. This is clearly shown in Figure 4.29. The effect of the input power on OSNR, signal power and noise power is compared and comprehensively shown in Table 4.5 where, as the input power level increases, the signal power also increases. Figure 4.29 where, as the input power level decreases, the noise power also decreases and Figure 4.30 where the threshold value of input power is found to be 40dBm below which the optical signal to noise ratio (OSNR) is constant.

4.7 Validation of the research work

1. Optical Infinite Impulse Response (Optical IIR) Filter

The Figure 4.31 a, shows the result of the work of Jain and Therese and fig. 4.31b, the proposed work. The four wave mixing sideband obtained by (Jain and Therese) was -69.6dBm and that

obtained in the proposed work is -99dBm. The performance of proposed work shows improvement over (Jain and Therese) because the FWM sideband obtained by (Jain and Therese) was -69.6Bm which is higher as compared to -99dBm, FWM sideband realized in this work (fig 4.31b). The reason of this performance is because of the incorporation of optical infinite impulse response (Optical IIR) filter in this work unlike in (Jain and Therese). This is due to the fact that the optical IIR filter is a recursive digital filter and also due to its efficiency and tolerance for loss. The optical IIR filter decomposes the desired filter response into a sum or difference of two all-pass filters. The filter responses are periodic, which is advantageous for WDM systems with more than one channel since the same filter can be used in different bands. The filter multichannel frequency selector has substantially better pass band flatness and stop band rejection than is possible with other filters having the same number of stages.

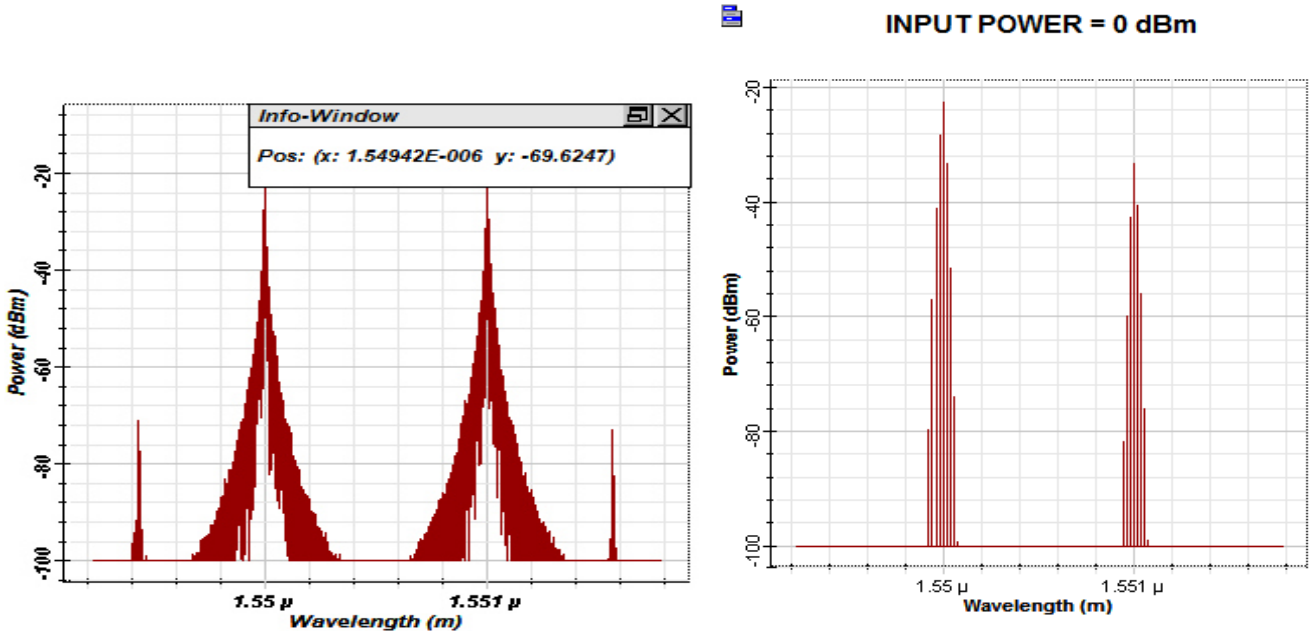

Fig 4.31 a) Jain and Therese **b) Proposed work**

Fig 4.31: Output Spectrums
Contribution = 42%

2. Dispersion Compensation Fiber and Fiber Bragg Grating (DCF+FBG)

The fig. 4.32a shows the result of the work of Jain and Therese and fig. 4.32b, the proposed work, the four wave mixing sideband obtained by (Jain and Therese) was -69.6dBm and that obtained in the proposed work is -85dBm. The performance of proposed work shows improvement over (Jain and Therese) because the FWM sideband obtained by (Jain and Therese) was -69.6Bm which is higher as compared to -85dBm FWM sideband realized in this work (fig 4.32b). The reason for this performance is because of the incorporation of dispersion compensation fiber and fiber bragg grating in this work unlike in (Jain and Therese). This is due to the fact that in the dispersion compensation fiber, the optical fiber component simulates the propagation of an optical field in a single mode fiber with the dispersive and nonlinear effects taken into account by a direct numerical integration of the modified nonlinear Schrodinger (NLS) equation and in the fiber bragg grating, the non-uniform grating is divided into number of segments uniform gratings. Also the apodized FBGs given better system performance than the conventional FBGs and FBGs have low insertion loss. The apodized grating play a very important role to suppress FWM sideband and maintaining the reflectivity and narrow bandwidth. According to fiber specification the chirp characteristics is readily chosen. To tolerate high optical power without any loss due to non-linear effect is prominent characteristics that separate the DCF and FBG from DCF. At low optical power the DCF show non-linearity effect, but at high power DCF and FBG would not introduce such effect in optical network.

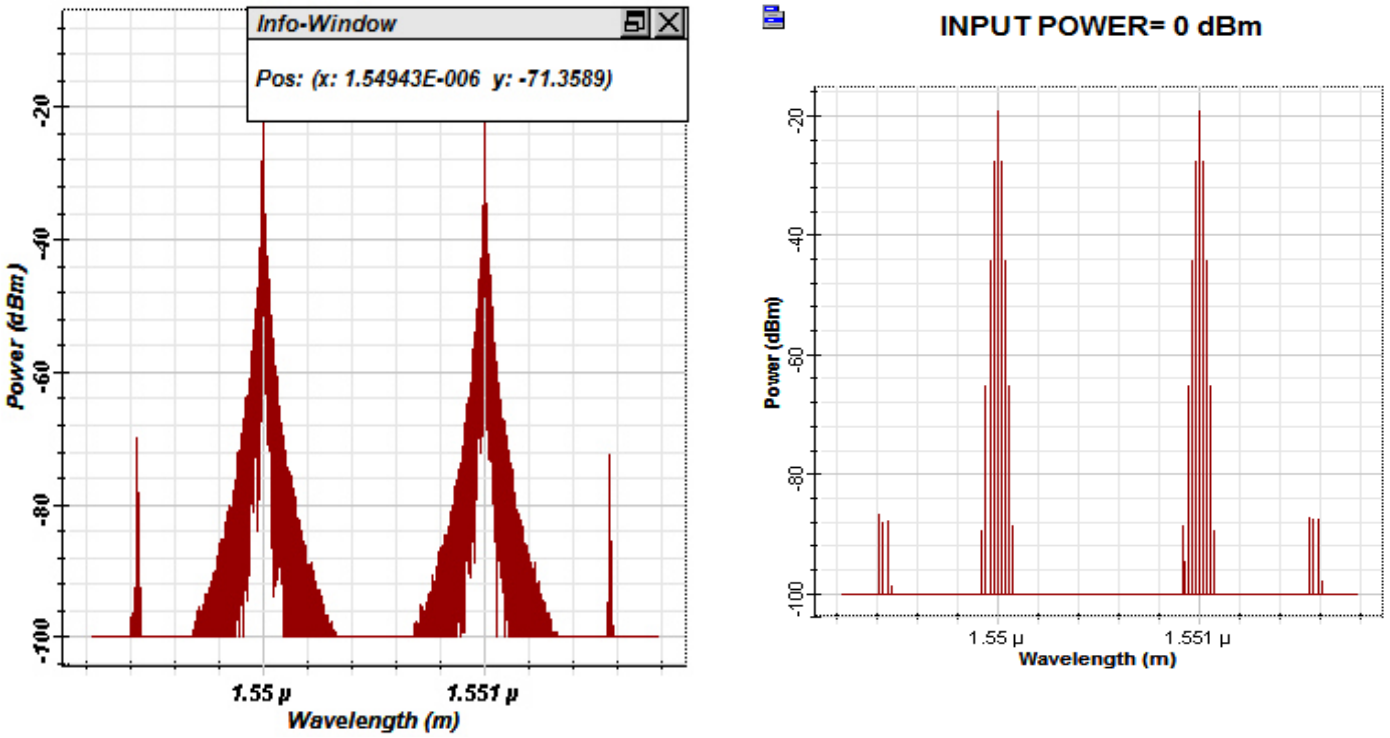

Fig. 4.32 a) Jain and Therese **b) Proposed work**

Fig 4.32: Output Spectrums
Contribution = 22%

3. Bessel Optical Filter (BOF)

The fig. 4.33a shows the result of the work of Jain and Therese and fig. 4.33b, the proposed work. The four wave mixing sideband obtained by (Jain and Therese) was -69.6dBm and that obtained in the proposed work is -84dBm. The performance of proposed work shows improvement over (Jain and Therese) because the FWM sideband obtained by (Jain and Therese) was -69.6Bm which is higher as compared to -84dBmFWM sideband realized in this work (fig 4.33b).The reason for this performance is because of the incorporation of bessel optical filter (BOF) in this work unlike in (Jain and Therese). This is due to the fact that the bessel optical filter is an optical filter with a bessel frequency transfer function and also due to the self-healing property of the bessel beam, the extended depth and tight focusing features of

the bessel beam. Also the bessel optical filter can automatically distinguish between the active wavelength and the newly generated wavelength by the algorithm programmed inside the filter which leads to a dramatic reduction in FWM. Also BOF drops multiple undesired frequencies that appear with the optical channels and BOF damp all FWM wavelengths in parallel that may appear with the main signals in the WDM system.

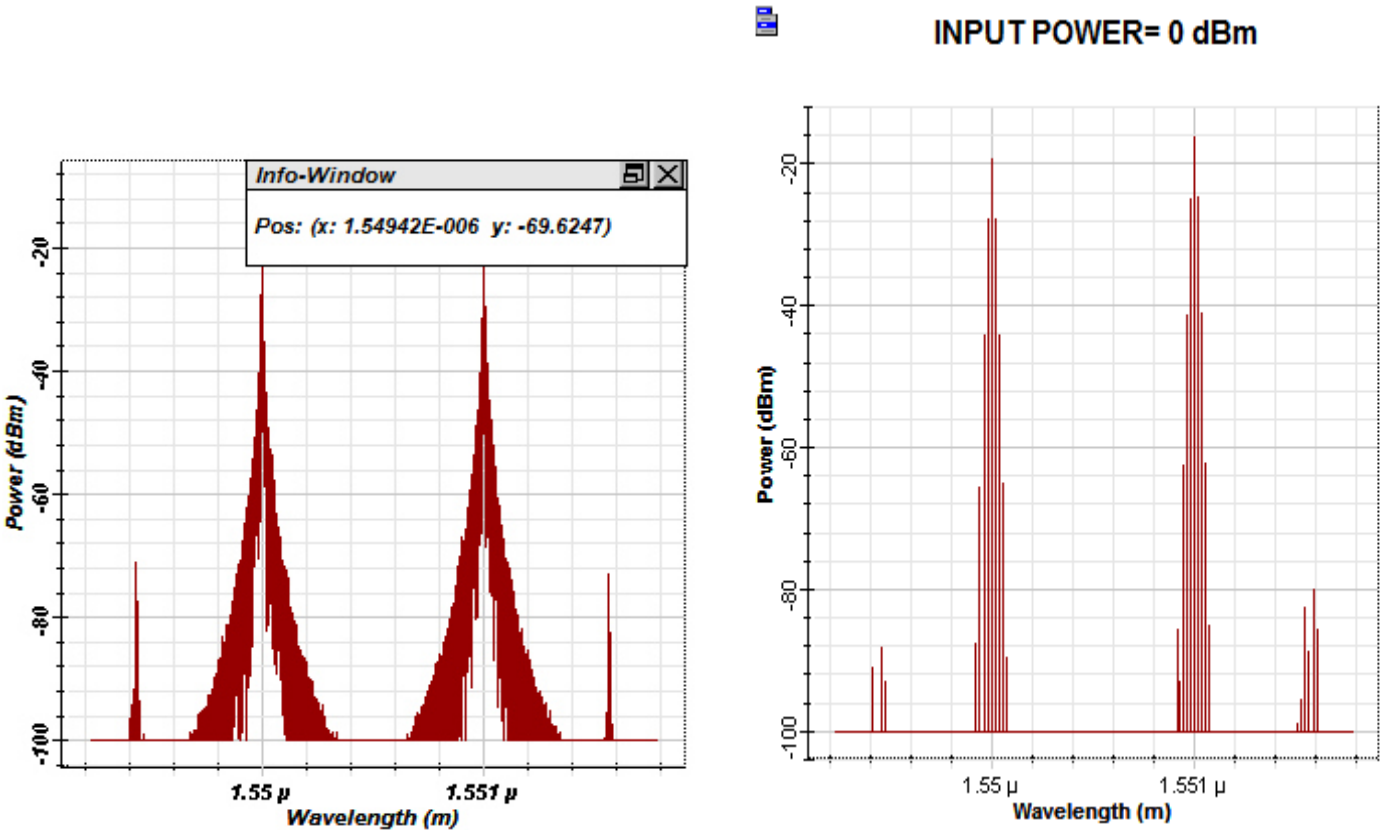

Fig. 4.33 a) Jain and Therese **b) Proposed Work**

Fig 4.33: Output Spectrums

Contribution = 21%

4. Polarization Controller (PC)

The fig. 4.34a shows the result of the work of Jain and Therese and fig. 4.34b, the proposed work. The four wave mixing sideband obtained by (Jain and Therese) was -69.6dBm and that obtained in the proposed work is -80dBm. The performance of proposed work shows

improvement over (Jain and Therese) because the FWM sideband obtained by (Jain and Therese) was -69.6dBm which is higher as compared to -80dBm FWM sideband realized in this work (fig 4.34b). The reason for this performance is because of the incorporation of polarization controller in this work unlike in (Jain and Therese). This is due to the fact that the polarization controller (PC) controls the state of polarization of light within the fiber core and then sets the input signal in an arbitrary polarization state. The polarization controller adjusts the first two incident waves to linear polarization. The PC controls the polarization angle between the pump light and the signal light. With the polarization controller most of the FWM frequencies were cancelled because the interaction between multiple optical channels that pass through the same fiber reduced, which suppressed the FWM.

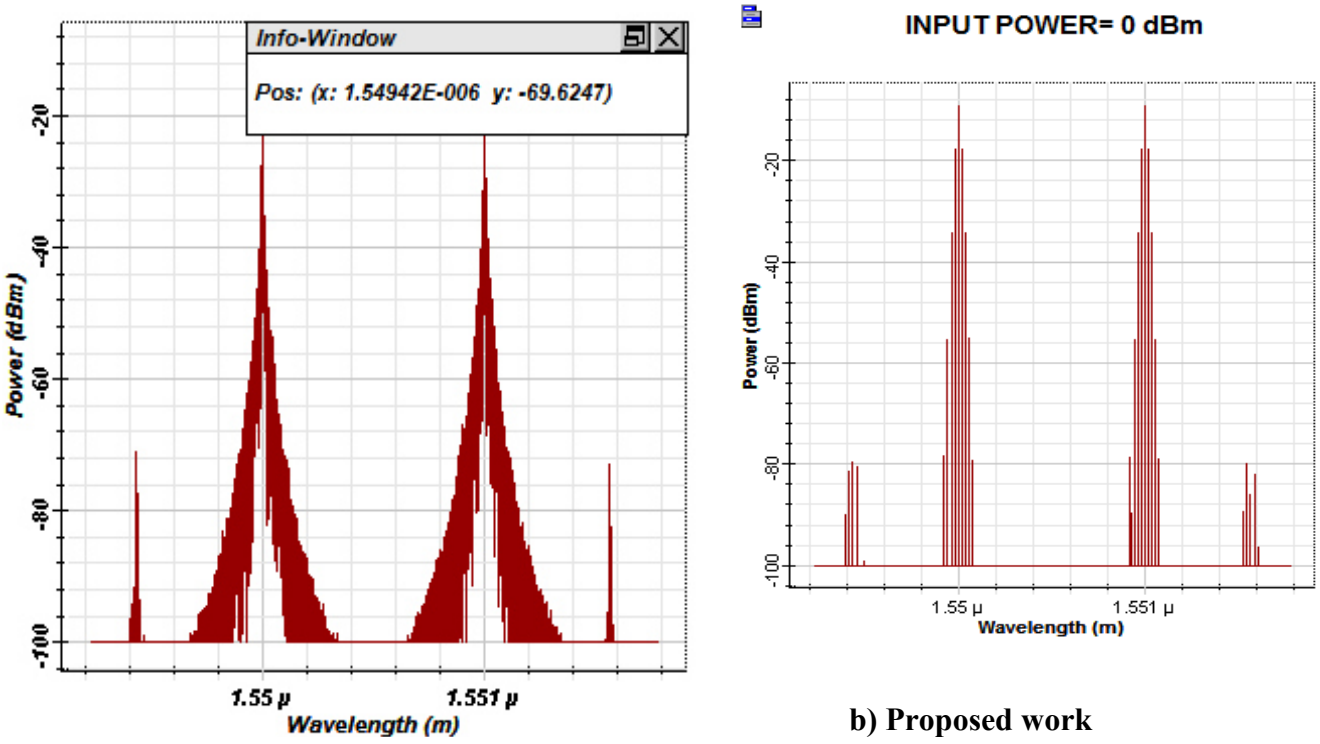

b) Proposed work

Fig 4.34: Output Spectrums
Contribution = 15%

1. Optical infinite impulse response (optical IIR) filter.

In the optical IIR filter, fig 4.35, the graphs of input signal power and noise power shows how large amount of noise was minimized from the system in the proposed work, -63dBm to -100dBm compared to the work of Jain and Therese, -60dBm to -92dBm, since FWM generates additional noise and degrades system performance and also, fig 4.36, the graphs of input signal power and OSNR, the optical signal to noise ratio for Jain and Therese (76dB) is slightly higher than that of the proposed work (70dB).

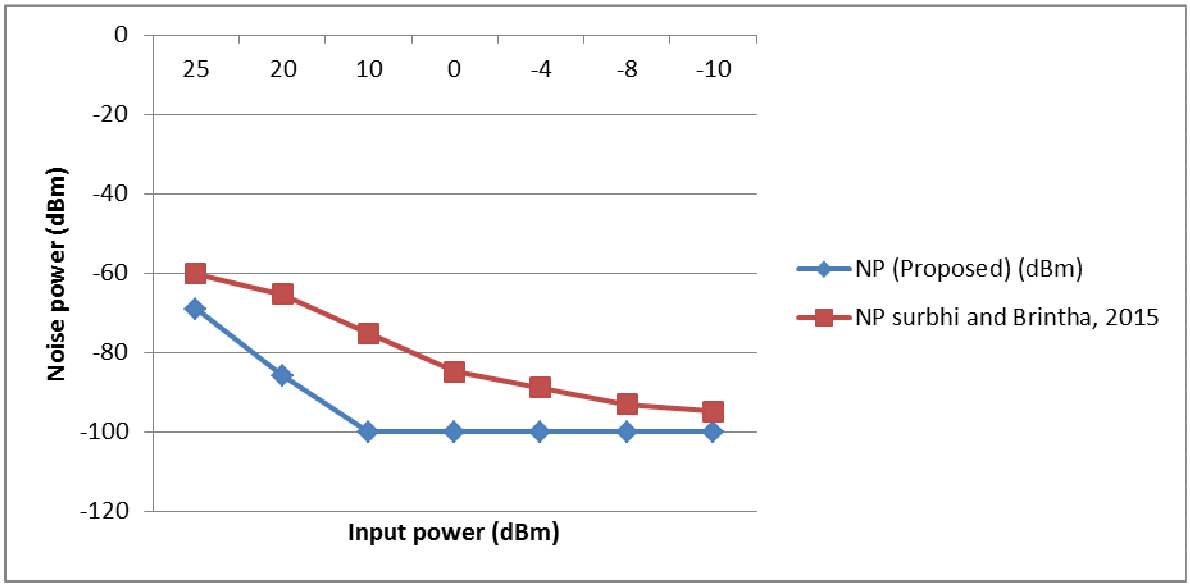

Fig. 4.35: Graphs of Input Signal Power and Noise power

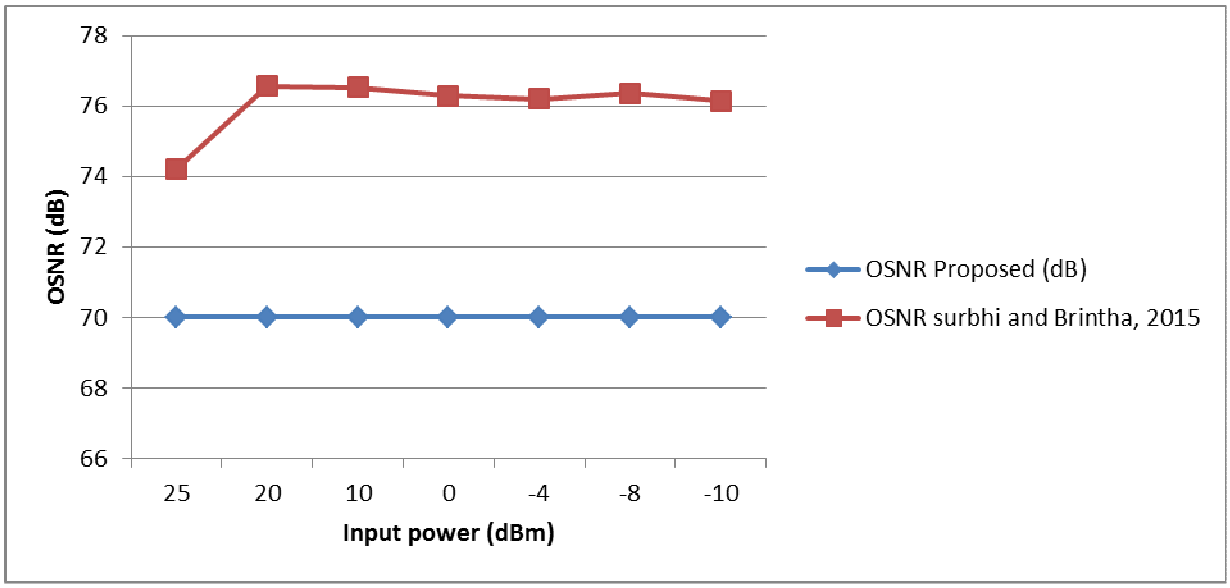

Fig. 4.36: Graphs of Input Signal Power and OSNR

2. Dispersion compensation fiber and Fiber bragg grating (DCF+FBG)

In the case of DCF+FBG, fig 4.37, the graphs of input signal power and noise power shows how large amount of noise was minimized from the system in the proposed work, -59dBm to -100dBm compared to the work of Jain and Therese, -18dBm to -88dBm, since FWM generates additional noise and degrades system performance and also, fig 4.38, the graphs of input signal power and OSNR, the optical signal to noise ratio for Jain and Therese (70dB) is slightly higher than that of the proposed work (65dB).

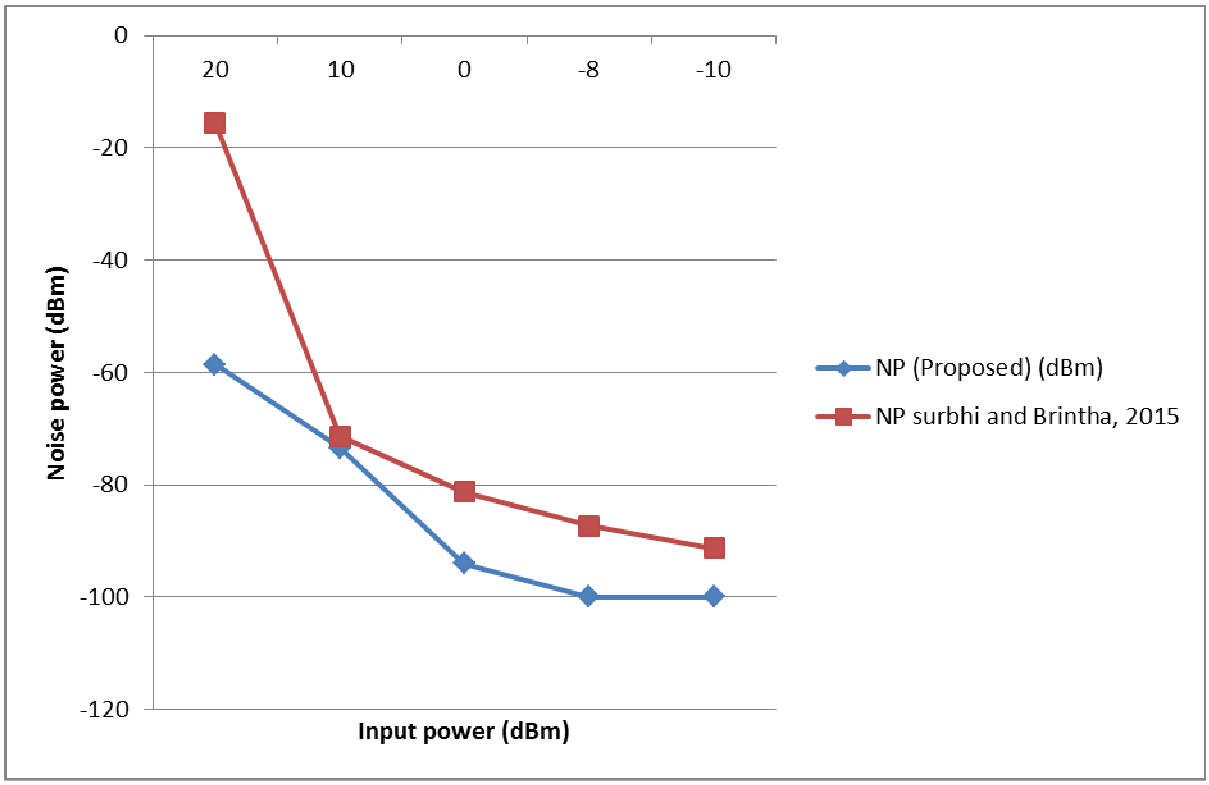

Fig. 4.37: Graphs of Input Signal Power and Noise power

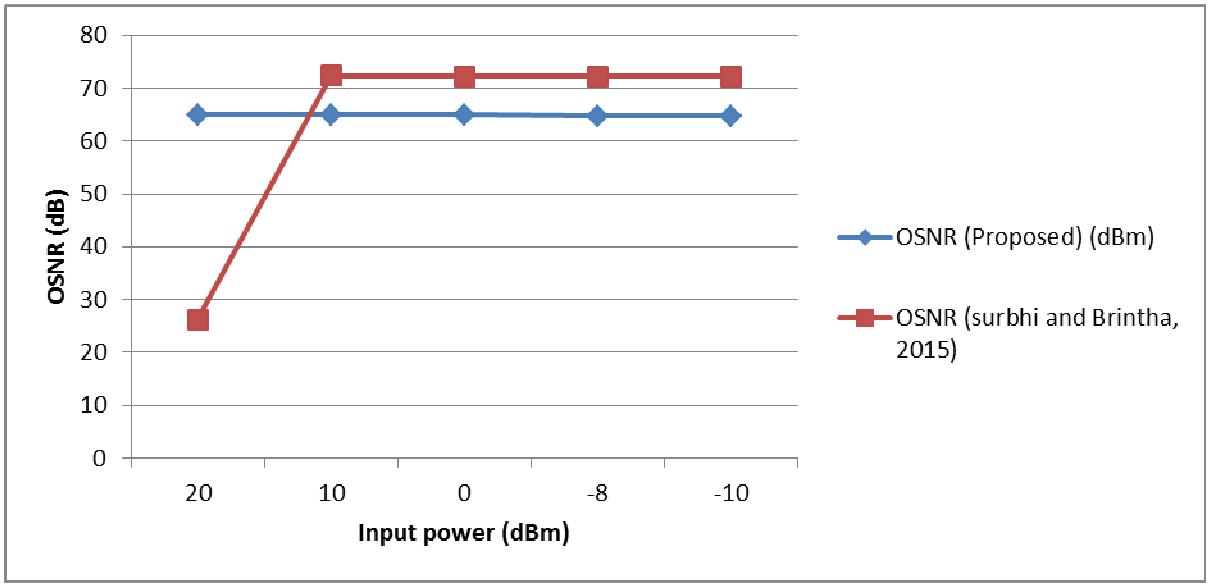

Fig. 4.38: Graphs of Input Signal Power and OSNR

3. Bessel optical filter (BOF)

In the BOF, fig 4.39, the graphs of input signal power and noise power shows how large amount of noise was minimized from the system in the proposed work, -61dBm to -100dBm compared to the work of Jain and Therese, -18dBm to -88dBm, since FWM generates additional noise and degrades system performance and also, fig 4.40, the graphs of input signal power and OSNR, the optical signal to noise ratio for Jain and Therese (72dB) is slightly higher than that of the proposed work (68.20dB).

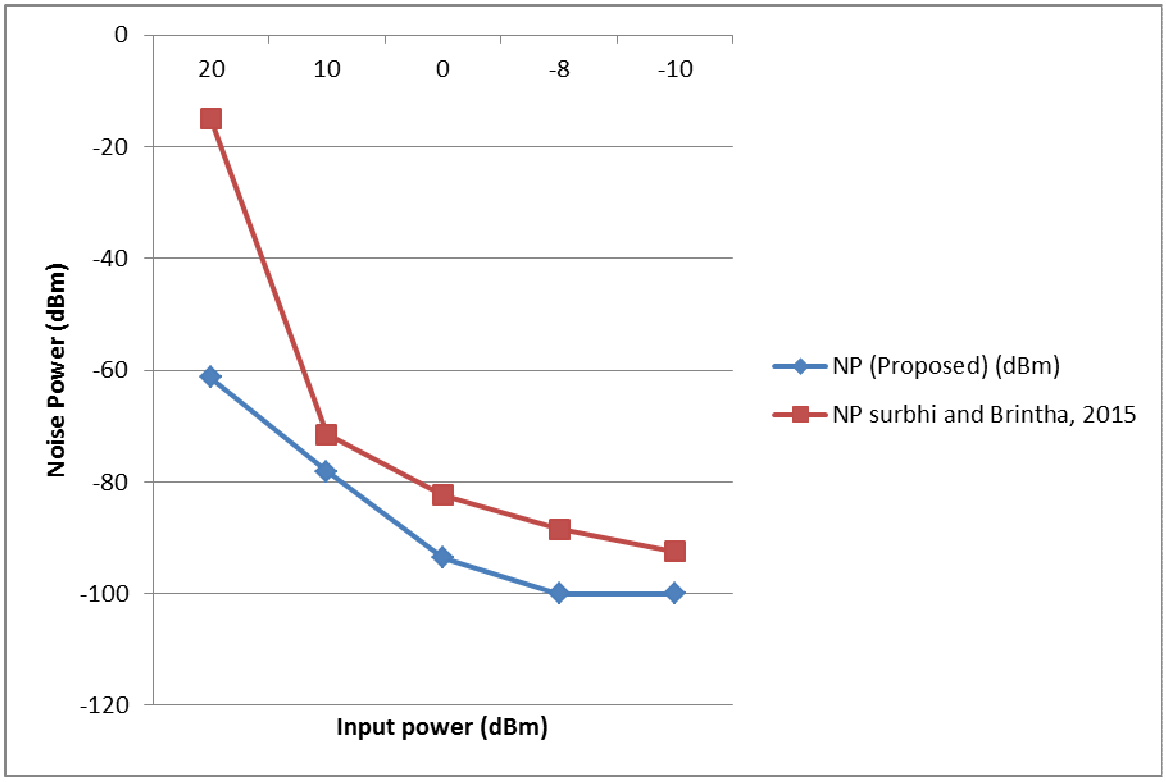

Fig.4.39: Graphs of Input Signal Power and Noise power

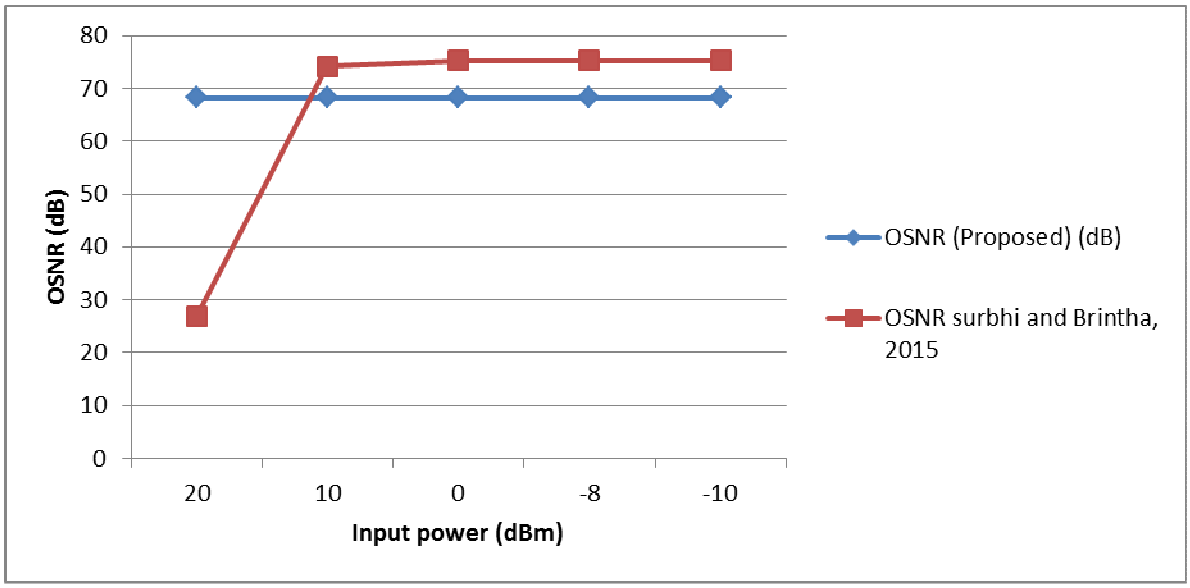

Fig. 4.40: Graphs of Input Signal Power and OSNR

4. Polarization controller (PC)

In the case of PC, fig 4.41, the graphs of input signal power and noise power shows how large amount of noise was minimized from the system in the proposed work, -42dBm to -100dBm compared to the work of Jain and Therese, -17dBm to -85dBm, since FWM generates additional noise and degrades system performance and also, fig 4.42, the graphs of input signal power and OSNR, the optical signal to noise ratio of proposed work (78.3dB) is higher than that of Jain and Therese (72dB).

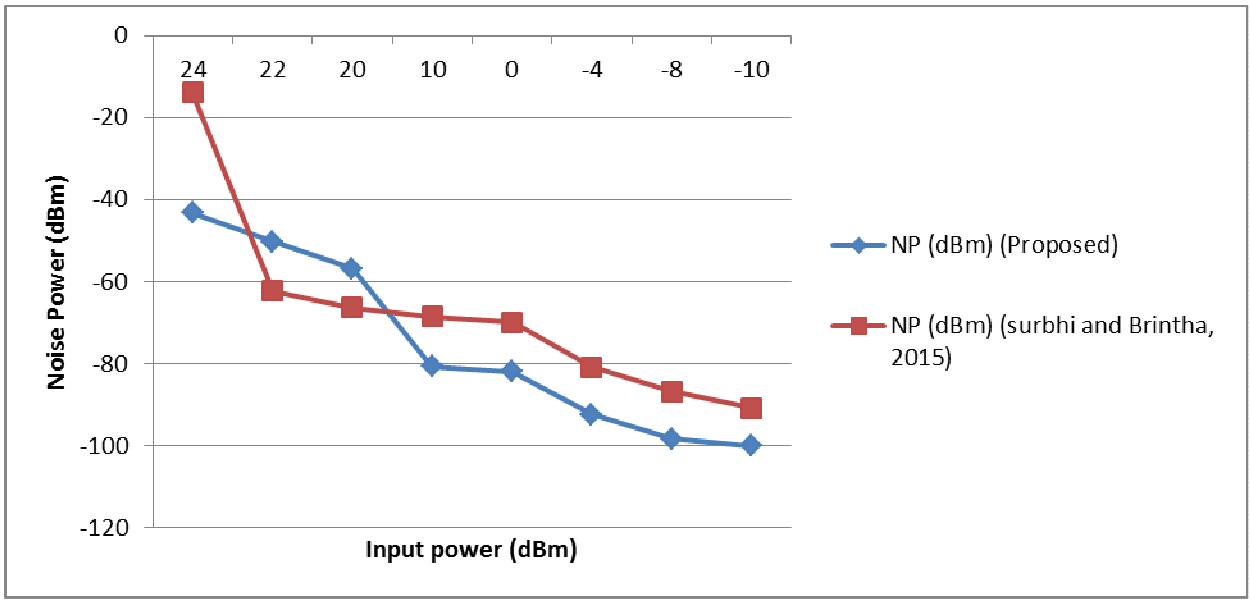

Fig. 4.41: Graph of Input Signal Power and Noise power

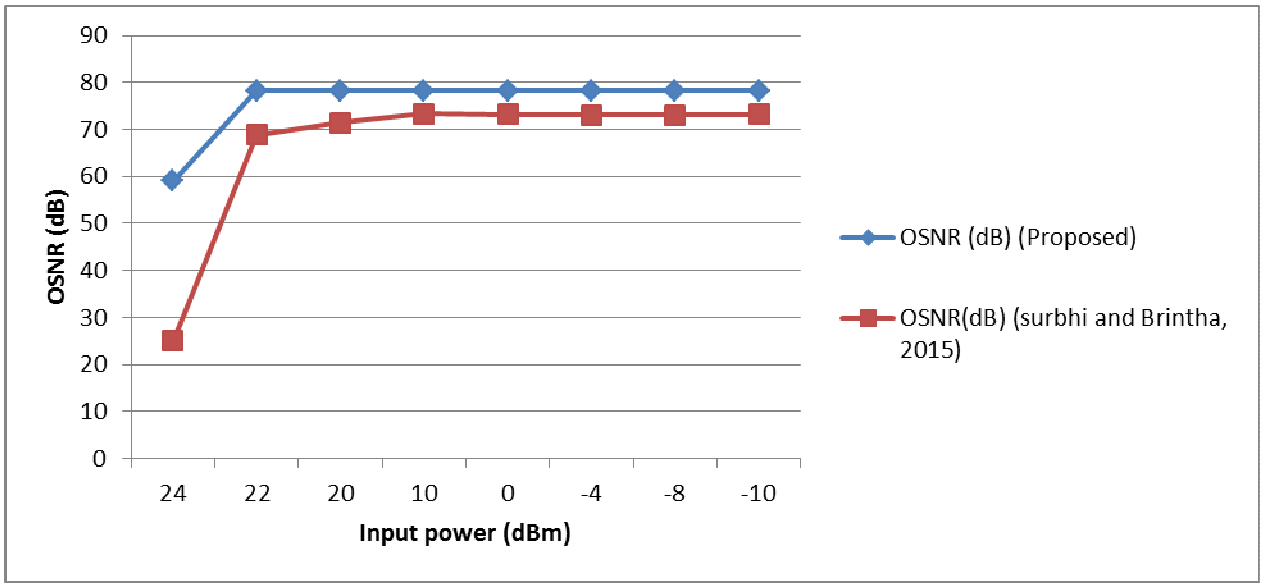

Fig. 4.42: Graph of Input Signal Power and OSNR

4.8 Major Contributions

Previously the best result obtained using duobinary modulation technique was that the four wave mixing sideband was reduced to -69.6dBm and the threshold value of input power obtained was 20 dBm.

In this research, after the simulation was performed the FWM effect has been minimized tremendously.

1. In the reduction of four wave nonlinearity effect in WDM systems using polarization controller. The FWM sideband was reduced to -80 dBm and the threshold value of input power obtained was 22dBm. A contribution of 15% when compared with the work of (Jain and Therese)
2. Also in the suppression of FWM effect in WDM systems using Bessel optical filter, the FWM sideband obtained was -84dBm and the threshold value of input power obtained was 27dBm. A contribution of 21% when compared with the work of (Jain and Therese)
3. The minimization of FWM effect using dispersion compensation fiber and fiber bragg grating the FWM sideband reduced to -85dBm and the threshold value of input power obtained was 30dBm. A contribution of 22% when compared with the work of (Jain and Therese)
4. Decreasing FWM nonlinearity effect in WDM systems using unequal channel spacing the FWM sideband was reduced to -88dBm and the threshold value of input power obtained was 30dBm. A contribution of 26% when compared with the work of (Jain and Therese).
5. Finally, the impact of optical infinite impulse response filter on the minimization of FWM effect resulted in reducing the FWM sideband to -99dBm and the threshold value of input power obtained was 40dBm which is the best result obtained. A contribution of 42% when compared with the work of (Jain and Therese).

CHAPTER FIVE

SUMMARY, CONCLUSION AND RECOMMENDATION

5.1 Summary

The future generation optical communication networks demand higher data rates. To achieve this, the nonlinear effect specifically four wave mixing need to be minimized if not completely corrected. In this research the incorporation of polarization controller, Bessel optical filter, dispersion compensation fiber and fiber bragg grating, unequal channel spacing technique and optical infinite impulse response filter in WDM system proved a better result in counteracting the effect of four wave mixing. The simulation was performed using optisystem, optical simulation software.

Reduction of four wave mixing nonlinearity effect in WDM system using polarization controller, the FWM sideband was reduced to -80dBm and the threshold value of input power obtained was 22dBm,suppression FWM in WDM system using Bessel optical filter, the four wave mixing sideband was reduced to -84dBm and the threshold value of input power obtained was 27dBm, minimization of FWM effect using dispersion compensation fiber and fiber bragg grating the FWM sideband was reduced to -85dBm and the threshold value of input power obtained was 30dBm,decreasing FWM nonlinearity effect in WDM system using unequal channel spacing the FWM sideband was reduced to -88dBm and the threshold value of input power obtained was 30dBm,finally, the impact of optical IIR filter (optical infinite impulse response filter) in correction of four wave mixing effect resulted in reduction of the FWM sideband to -99dBm and the threshold value of input power obtained is 40dBm,the threshold value of input power is the input power level below which the optical signal to noise ratio is constant.

5.2 Conclusion

In conclusion, not like the linear effects which can be replaced, the nonlinear effects become more and degrade the system performance. The capacity of information of a light wave is majorly limited by the nonlinear interactions between the information signals and the fiber medium. Four-Wave Mixing (FWM) is a type of nonlinear effect which occurs in wavelength division multiplexing (WDM) when light of two or more different wavelengths are launched into a fiber. FWM is a main source of nonlinear crosstalk since they interfere with the desired signals. The effect of four wave mixing (FWM) as one of the key factors in the WDM has been studied here using optisystem. The investigation of FWM effect for various parameters has been done. The four wave mixing effect has been minimized.

5.3 Recommendation

Further work can be done to reduce the four wave mixing (FWM) effect at high input power levels.

References

[1] S. Kothari, K. Jaiswal, S. Vijayvargiya, and A. Jabeena, "Analysis of four wave mixing in WDM optical fiber systems using labview," ARPN Journal of engineering and applied sciences,vol.9,no.8,2014.

[2] D.P. Mishra and A. Panda, "Nonlinear effect of four wave mixing for WDM in radio-over-fiber systems," Journal of electronics and communication engineering research,vol.2(4),2014.

[3] M. Singh and V. Sharma, "Investigation of four wave mixing effect at different transmission power levels and channel spacing," International journal of computer applications, vol.128 (1),pp.12-17,2015.

[4] V. Kaur and K.S. Bhatia, "Suppress the FWM by increasing channel spacing and chromatic dispersion of fiber in WDM system, "J. opt. commun.,2015.

[5] S. Jain and A.B. Therese, "Reduction of four wave mixing non-linearity effect in WDM radio over fiber systems, "Journal of science and technology,vol.8(19),2015.

[6] H.J. Abed, N.M. Din, M.H. Al-Mansoori, F. Abdullah, and H.A. Fadhil, "Four wave mixing suppression in optical systems through system parameters optimization," Research journal of applied sciences, engineering and technology, vol.7(15),pp.3010-3014,2014.

[7] D. Bhalla and M. Bhutani, "Performance analysis of four wave mixing: A non-linear effect in optical fibers," Journal of computer applications, vol.93 (7), 2014.

[8] S.E Jenifa and K. Gokulakrishnan, "Performance measures of DWDM system under the impact of four wave mixing," International journal of scientific engineering and research, vol.3 (5), 2015.

[9] A. Panda and D.P Mishra, "Effect of four wave mixing in WDM systems for higher number of channels," International journal of smart sensors and adhoc networks, vol.3 (1), 2013.

[10]S. P. Vashisht, S. Sugumaran, S. Agarwal, A. Mukherjee, and P. Karmakar, "Analysis of four wave mixing in WDM optical systems," 2014.

[11]K.N. Ali, "Four wave mixing non linearity effect in wavelength division multiplexing radio over fiber system," Journal of engineering sciences, vol. 6(2), pp. 204-230, 2013.

[12]R. Kaur and S. Dewra, "Duobinary modulation format for optical system – A review," International journal of advanced research in electrical, electronics and instrumentation engineering, vol.3(8), pp. 11039- 11046, 2014.

[13]H. U. Manzoor, T. Manzoor, and T. Mehmood, "Reduction of four wave mixing by employing circular polarizers in DWDM optical networks," Research gate, pp-637-640, 2015.

[14]I. Tiwari, S. Garg, V. Kawatra, B. Sridhar, and M. Bhutani, "Effect of different modulation formats on DWDM optical transmission systems in the presence of four wave mixing," International journal of enhanced research in science, technology and engineering, vol.4(3), 2015.

[15]F. Dehghani and F. Emami, "Suppression of four wave mixing based on the pairing combinations of differently linear polarized optical signals in WDM system," Journal of optoelectronical nanostructures, vol. 1 (1), 2016.

[16]A. K. Goel and N. Singh, "Analysis of four wave mixing effect at different channel spacing in DWDM systems using EDFA with single pump source," International journal of engineering sciences, vol.17, pp. 382-388,2016.

[17]J. Kaurand H. Singh, " Investigation of four wave mixing in high capacity and high speed WDM system," International journal of engineering development and research, vol.5(2), pp.1362-1368, 2017.

[18]A. Chadha, N. Satam, S. Mehta, and S. Jagtap, "Performance analysis of WDM-based optical communication systems in presence of Kerr nonlinearities," International journal of current engineering and technology, vol.7 (2), pp.620-628, 2017.

[19] R. Erdogan, "Fiber grating spectra," J. Light Technol., vol. 15, pp.1277-1294,1997.

[20] G.P. Agrawal, "Applications of nonlinear fiber optics," 3rdEdn., Academic press, 2011.

[21] S.P. Singh and N. Singh, "Non-linear effects: progress in electromagnetic research," vol.73, pp. 249-275, 2007.

[22] M. Ajiya, "Fiber losses and nonlinear effects in optical fibers," vol.5, pp.24-39, 2015.

[23] Maxim Integrated, "Optical signal-to-noise ratio and the Q-factor in fiber-optic communication systems," 2016.

[24] T. Schneider, "Nonlinear optics in telecommunications,"4thEdn., Academic press, pp. 123-145, 2013.

[25] R.W. Boyd, "Nonlinear optics," Academic press, San Diego, CA, 1992.

[26] R.W. Boyd, "Nonlinear optics," Third edition, Academic press, San Diego, CA, 2007.

[27] J.C Palais, " Fiber optic communications," Third Edition, Prentice Hal., 1998.

[28] W.H. Press, B.P. Flannery, S.A Teukolsky, and W.T. Vetterling, Numerical Recipes Inc., Cambridge university press, 2003.
[29] OPTIWAVE, “Optical System User’s Reference Optical Communication System Design Software Version 13,” 2014.